DOI: 10.1002/cmdc.200800043

Development of Benzophenone-Based Farnesyltransferase Inhibitors as Novel Antimalarials

Katja Kohring,[a] Jochen Wiesner,[b] Mirko Altenkämper,[a] Jacek Sakowski,[a] Katrin Silber,[a] Alexander Hillebrecht,[a] Peter Haebel,[a] Hans-Martin Dahse,[c] Regina Ortmann,[a] Hassan Jomaa,[b] Gerhard Klebe,[a] and Martin Schlitzer*[a]

The development of farnesyltransferase inhibitors directed against Plasmodium falciparum *is a strategy towards new drugs against malaria. Previously, we described benzophenone-based farnesyltransferase inhibitors with high in vitro antimalarial activity but no in vivo activity. Through the introduction of a methylpiperazinyl moiety, farnesyltransferase inhibitors with in vivo antimalarial activity were obtained. Subsequently, a structure-based design approach was chosen to further improve the antimalarial activity of this type of inhibitor. As no crystal structure of the farnesyltransferase of the target organism is available, homology modeling was used to reveal differences between the active sites of the rat/human and the* P. falciparum *farnesyltransferase. Based on flexible docking data, the piperazinyl moiety was replaced by a* N,N,N′*-trimethylethylenediamine moiety. This resulted in an inhibitor with significantly improved in vitro and in vivo antimalarial activity. Furthermore, this inhibitor displayed a notable increase in selectivity towards malaria parasites relative to human cells.*

Introduction

Farnesyltransferase has been one of the prime targets in the development of novel anticancer agents, due to the observation that many proteins involved in intracellular signal transduction are substrates of this enzyme. Several farnesyltransferase inhibitors have reached advanced stages of clinical trials.[1–9] Farnesyltransferase catalyzes the transfer of a farnesyl residue from farnesyl diphosphate to the thiol of a cysteine side chain of proteins carrying the CAAX-tetrapeptide sequence (C: cysteine, A: aliphatic amino acid, X: serine or methionine) at their C terminus.[10,11] Most previous experiments were performed with recombinant farnesyltransferase from human, rat, or yeast. There are no structural differences between the active sites of the human and the rat farnesyltransferase, and also the active-site geometry of the yeast enzyme is highly related to the mammalian homologues. Farnesyltransferases were also identified in other eukaryotic organisms including the pathogenic protozoa *Plasmodium falciparum,*[12,13] *Trypanosoma brucei,*[14–16] *T. cruzi,*[17] *Leishmania major,*[17] *Toxoplasma gondii,*[18] and *Entamoeba histolytic*a.[19] Therefore, inhibition of the farnesyltransferase has also been suggested as a new strategy for the treatment of parasitic infections.[2] The most important of these protozoa-related diseases is malaria tropica caused by the infection with *P. falciparum*. Approximately 40% of the world's population live in areas with malaria risk, and two to three million people die each year from malaria. As a result of the increasing spread of malaria parasites resistant to chloroquine and other commonly used antimalarials, there is an urgent need for new therapeutics.[20,21] All efforts towards the heterologous expression of the farnesyltransferase gene from *P. falciparum* have failed so far and, therefore, no recombinant enzyme is available for routine screening. Only the native protein has been purified from in vitro parasite cultures and used to demonstrate its inhibition by farnesyltransferase inhibitors.[12,13] However, for the development of new chemotherapeutics, growth inhibition data obtained with cultured blood stages of the parasite seem to be more significant. For example, Chakrabarti et al. have demonstrated subnanomolar activity for a farnesyltransferase inhibitor derived from the groups of Sebti and Hamilton against the isolated FTase from *P. falciparum* but reported only micromolar activity of this compound against cultured *P. falciparum* blood forms.[13] During the last years we have developed a new class of farnesyltransferase inhibitors based on a benzophenone scaffold.[23] Compounds of this type suppress the growth of the multiresistant *P. falciparum* strain Dd2 in the nanomolar range.[24–27] To our disappointment, such inhibitors with high in vitro potency turned out to be inactive in a murine malaria model. We speculated that the lack of in vivo activity was caused by insufficient solubility of the inhibitors. Therefore, we introduced nitrogen con-

[a] *Dr. K. Kohring, M. Altenkämper, Dr. J. Sakowski, Dr. K. Silber, Dr. A. Hillebrecht, Dr. P. Haebel, Dr. R. Ortmann, Prof. Dr. G. Klebe, Prof. Dr. M. Schlitzer*
Institut für Pharmazeutische Chemie
Philipps-Universität Marburg, Marbacher Weg 6, 35032 Marburg (Germany)
Fax: (+49) 6421-282-5953
E-mail: schlitzer@staff.uni.marburg.de

[b] *Dr. J. Wiesner, Priv.-Doz. Dr. H. Jomaa*
Instiut für Klinische Chemie und Pathobiochemie
Universitätsklinikum Gießen und Marburg, Gaffkystraße 11, 35392 Gießen (Germany)

[c] *Dr. H.-M. Dahse*
Leibniz-Institut für Naturstoff-Forschung und Infektionsbiologie
Hans-Knöll-Institut, Beutenbergstraße 11, Jena (Germany)

Supporting information for this article is available on the WWW under http://www.chemmedchem.org or from the author.

taining substituents capable of switching between a protonated and a non-protonated state within a physiological pH range, finally leading to the first farnesyltransferase inhibitors with in vivo antimalarial activity.[28]

Results and Discussion

Chemistry

For the synthesis of the phenylacetic acid derivatives **8**, 2-amino-5-nitro-benzophenone **4** was acylated with commercially available α-chlorophenyl acetyl chloride **3**. Subsequently, the α-chlorine of compounds **5** was substituted by different heterocyclic secondary amines yielding the intermediates **6**. After reduction of the nitro group, yielding amines **7**, a second acylation step with the 3-[5-(4-nitrophenyl)-2-furyl]acrylic acid resulted in the target compounds **8** (Scheme 1). For the synthesis of the *para*-chlorophenylacetic acid derivative **13**, 4-chlorophenylacetic acid **9** was first α-brominated and then transformed into the corresponding acid chloride **10**. Then, the synthesis continued as outlined above using *N*-methylpiperazine as the N-heterocycle (Scheme 2). Preparation of homologue **18** was achieved accordingly starting with the α-bromination of 4-chlorophenylpropionic acid **14** (Scheme 2). Synthesis of the *N,N,N′*-trimethylethylenediamine derivatives **20** and **22** started from the intermediates **5** and **11**, respectively, which were first reacted with *N,N,N′*-trimethylethylenediamine yielding the intermediates **19** and **21**. Reduction of the nitro group and acylation of the resulting amino group yielded the target compounds as described above (Scheme 3). The *N,N,N′*-trimethyltrimethylenediamine compounds **23** and **24** were prepared in the same way using *N,N,N′*-trimethyltrimethylene-1,3-diamine instead of *N,N,N′*-trimethylethylenediamine.

Farnesyltransferase inhibition assay

The inhibitory activity of the inhibitors was determined using the fluorescence enhancement assay as described by Pompliano.[29] The assay employs yeast farnesyltransferase (FTase) fused to glutathione *S*-transferase at the N terminus of the β-subunit.[30] Farnesylpyrophosphate and the dansylated pentapeptide Ds-Gly-Cys-Val-Leu-Ser were used as substrates. Upon farnesylation of the cysteine thiol the dansyl residue is placed in a lipophilic environment resulting in an enhancement of fluorescence at 505 nm which is used to monitor the enzyme reaction.

In vitro and in vivo antimalarial activity

Compounds were assayed for their inhibitory activity against intraerythrocytic forms of the *P. falciparum* strain Dd2 using a semiautomated microdilution assay as described.[31–33] The growth of the parasites was monitored through the incorporation of tritium-labeled hypoxanthine. The Dd2 strain is resistant to several commonly used antimalarial drugs (chloroquine, cycloguanil, and pyrimethamine) (see Table 2 below). The comparability of measurements of different series was granted by concurrent assay of standard compounds.

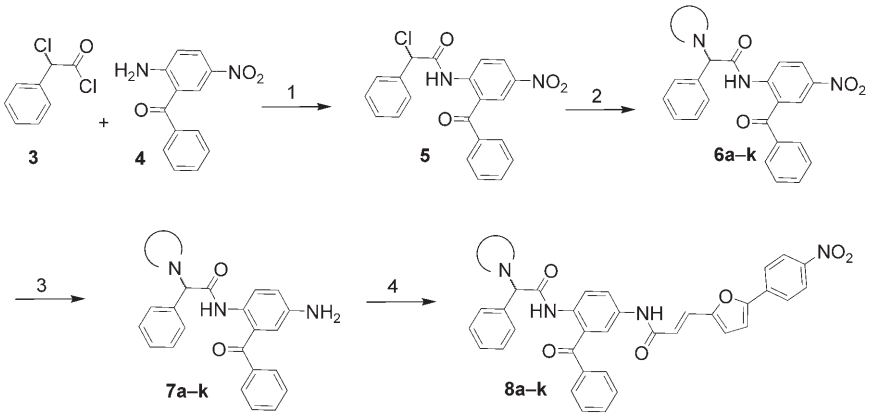

Scheme 1. Reagents and conditions: 1) toluene/dioxane, reflux, 2 h; 2) (4-oxo)piperidine or morpholine or N-substituted piperazine, acetonitrile, reflux, 24 h; 3) $SnCl_2 \cdot 2H_2O$, ethyl acetate, reflux, 2 h; 4) 3-[5-(4-nitrophenyl)-2-furyl]acrylic acid, toluene/dioxane, reflux, 2 h.

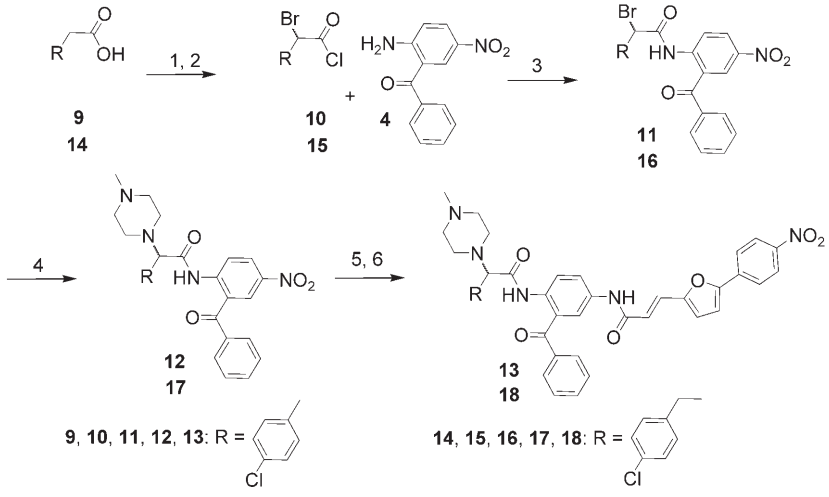

Scheme 2. Reagents and conditions: 1) bromine, benzene, reflux, 1–3 days; 2) oxalylchloride, dichloromethane, RT, 2 h; 3) toluene/dioxane, reflux, 2 h; 4) *N*-methylpiperazine, acetonitrile, reflux, 24 h; 5) $SnCl_2 \times 2H_2O$, ethyl acetate, reflux, 2 h; 6) 3-[5-(4-nitrophenyl)-2-furyl]acrylic acid, toluene/dioxane, reflux, 2 h.

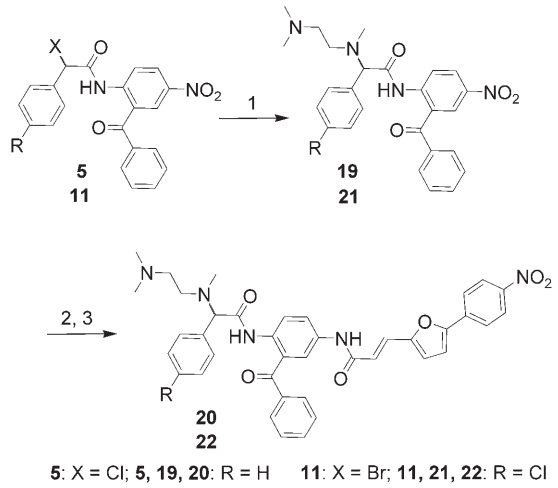

Scheme 3. Reagents and conditions: 1) *N,N,N′*-trimethylethylenediamine, acetonitrile, reflux, 24 h; 2) $SnCl_2 \cdot 2H_2O$, ethyl acetate, reflux, 2 h; 3) 3-[5-(4-nitrophenyl)-2-furyl]acrylic acid, toluene/dioxane, reflux, 2 h.

The in vivo testing was carried out according to a modified standard protocol (Peter's test) using *P. vinckei* infected mice.[34] On day 0 Balb/c mice were infected with 5×10^7 parasites from the blood of a donor mouse. On day one to three the mice were treated by intraperitoneal (i.p.) injection of the test substance with dosages of 6, 13, 25, and 100 mg kg^{-1} bw (body weight) once a day. On day four the parasitemia (percentage of infected erythrocytes) was counted microscopically on Giemsa-stained blood smears.

Flexible docking

The protein structure was taken from the PDB entry 1QBQ.[22] Ligands and solvent molecules were removed, but the zinc ion and farnesyl diphosphate were included as part of the protein. Docking was performed using AutoDock 3.0.[35,36] Docking solutions from 50 individual runs were clustered using a mutual rmsd < 1 Å as criterion and represented by the conformer with the best docking energy.

Homology modeling

A homology model of *P. falciparum* farnesyltransferase was prepared to analyze the differences between mammalian and parasite enzymes. Sequences for α and β subunits of rat (Q04631 and Q02293) and *P. falciparum* (Q8I503 and Q8IHP6) farnesyltransferase were retrieved from SWISS-Prot[37] and aligned with T-COFFEE.[38] *P. falciparum* homology models were computed based on the alignments and the rat template structure (PDB entry: 1QBQ) using MODELLER.[39] The sequence for farnesyltransferase from *P. vinckei* is not known.

ADME parameters

All molecules have been built using MOE, basic nitrogens were assumed as protonated. After calculation of charges according to the MMFF94x force field 45 simple two-dimensional molecular descriptors have been computed such as molar refraction, log *P*, number of rotatable bonds, and many descriptors related to distinct fractions of the van der Waals surface area subdivided according to polarity.

Cytotoxicity assay

Cytotoxicity of selected compounds was evaluated against HeLa cells. Viability of the cells was determined after a 72 h incubation period using methylene blue staining and photometric evaluation.

Results

The starting point for our attempt to obtain farnesyltransferase inhibitors with in vivo activity was the inhibitor **1a**. Several different nitrogen-containing heterocycles were introduced into the α-position of the phenylacetic acid substructure of this compound. Through this modification, water solubility was considerably enhanced from < 0.06 mM for phenylacetic acid derivative **1a** to > 3.33 mM for the piperazine analogue **8d**.[28] Into the α-position of the phenylacetic acid substructure of this compound several different nitrogen-containing heterocycles were introduced. Of the 11 derivatives **8a**–**k** obtained that way, four displayed antiparasitic activity comparable to the lead structure **1a** ($IC_{50} = 270$ nM) (Table 1). Three of them are piperazine derivatives carrying a methyl (**8d**: $IC_{50} = 270$ nM), a hydroxyethyl (**8g**: $IC_{50} = 270$ nM), and a cyclohexyl (**8i**: $IC_{50} = 200$ nM) residue, respectively at the N4 of the piperazine moiety. However, the presence of a second nitrogen is not mandatory as demonstrated by the morpholinyl derivative **8c** ($IC_{50} = 320$ nM). Notably, the *N*-ethyl derivative **8e** is considerably less active than the methyl (**8d**) or the propyl derivative **8f**. As molecular descriptors of these three molecules do not vary that much (vide infra), we attribute this to minor differences in the structure of the farnesyltransferase which cannot be accessed by homology modeling. This interpretation is supported by results we reported earlier on the activity of these compounds against *Trypanosoma cruzi*[54] where the ethyl derivative **8e** is also considerably less active than the methyl **8d** and propyl derivative **8f**, whereas against *T. brucei*, the ethyl derivative **8e** is more active than the propyl homologue **8f** (unpublished results). Farnesyltransferase inhibitory activity varied considerably within this series and showed no obvious correlation with the antimalarial activity. However, when comparing farnesyltransferase inhibitory and antimalarial activity one has to take into account that *P. falciparum* farnesyltransferase is not available for routine screening and that farnesyltransferase from yeast used in this study more closely resembles human FTase than *Pf*FTase and therefore, a straightforward correlation between FTase inhibition and antimalarial activity may not be expected. As novel starting point for further development the methylpiperazinyl-substituted inhibitor **8d** was selected because of its high activity and relative structural simplicity. As hoped for, inhibitor **8d** demonstrated in vivo activity in the *P. vinckei* infected mouse. ED_{50} and ED_{90} values were determined as 45 μmol (30 mg) kg^{-1} bw and 65 μmol (40 mg)

Table 1. In vitro antiplasmodial activity[a] and farnesyltransferase inhibition of compounds **8a–k**.

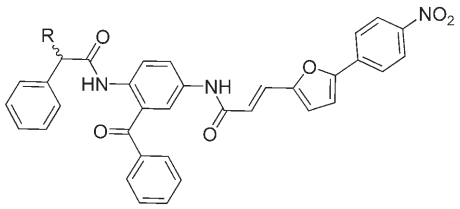

Compd	R	IC_{50} [nM] FTase	IC_{50} [nM] *P. falciparum*	Compd	R	IC_{50} [nM] FTase	IC_{50} [nM] *P. falciparum*
8a		453 ± 33	1500	**8b**	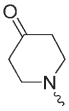	1093 ± 97	2000
8c		660 ± 100	320	**8d**	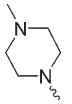	10 ± 3	270
8e	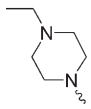	> 10000	3000	**8f**	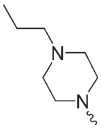	123 ± 11	630
8g	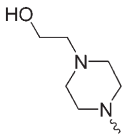	430 ± 60	270	**8h**	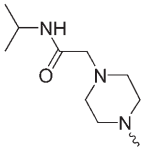	338 ± 45	490
8i	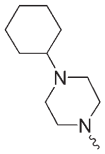	339 ± 80	200	**8j**	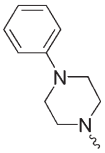	297 ± 66	3100
8k	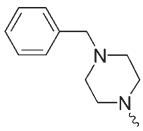	660 ± 56	670				

[a] IC_{50} values (nM) for standard antimalarials were: chloroquine, 170; pyrimethamine, 2500; cycloguanil, 2200; quinine, 380; lumefantrine, 30; artemisinin, 18.

kg^{-1} bw, respectively (Table 2). As in the case of the α-unsubstituted inhibitors **1a** and **b**, the introduction of a chlorine substituent into the *para*-position of the terminal phenyl residue resulted in a considerable enhancement in in vitro activity (shown) the same modification was done for the inhibitor **8d** yielding compound **13** (Table 2). Although this modification resulted in an enhancement in in vitro activity also in the case of the methylpiperazinyl-substituted compound, the effect was considerably less pronounced than in the case of the α-unsubstituted inhibitors **1a** and **b** with an IC_{50} value of 210 nM for **13**. However, an improvement in in vivo activity in the mouse model with ED_{50} and ED_{90} values of 30 μmol (21 mg) kg^{-1} bw and 36 μmol (25 mg) kg^{-1} bw, respectively (Table 2) could also be recorded. In vitro cytotoxicity was similar for both inhibitors **8d** and **13** giving a CC_{50}/IC_{50} ratio of 137 and 184, respectively. Toxic effects were seen in vivo only at doses higher than 100 mg kg^{-1} bw. The mechanism of action of these type of inhibitors was confirmed by monitoring the farnesylation level of parasite proteins after metabolic labeling with

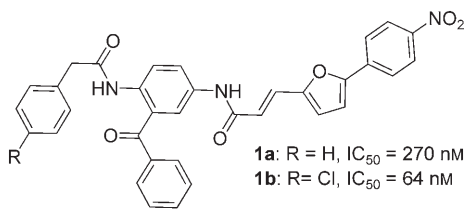

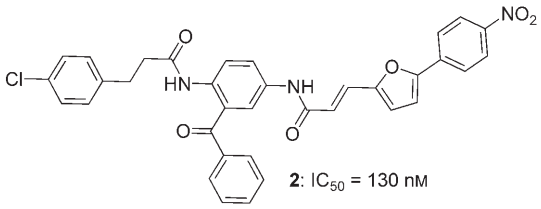

Table 2. Activity of N-methylpiperazine-substituted compounds **8d**, **13**, and **18**.

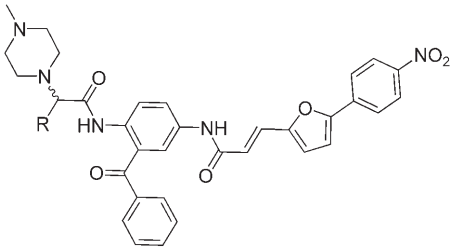

Compd	R	IC_{50} [nM] FTase	IC_{50} [nM] *P. falciparum*	ED_{50} [μmol kg^{-1}] (mg kg^{-1}) *P. vinckei*	ED_{90} [μmol kg^{-1}] (mg kg^{-1}) *P. vinckei*	CC_{50} [nM] HeLa	CC_{50}/IC_{50}
8d		10±3	270	45 (30)	60 (40)	37.0	137
13	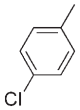	4±2	210	30 (21)	36 (25)	38.6	184
18	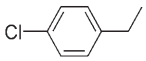	124±15	210	nd[a]	nd	18.0	86

[a] Not determined

[^{3}H]farnesylpyrophosphate using the technology previously described by Chakrabarti[13] and Katzin.[40] In the presence of inhibitor **13** the protein farnesylation was significantly reduced in all *P. falciparum* blood stages.[28]

A possible explanation for the comparatively low enhancement in activity associated with the introduction of the chlorine residue as well as some clues for further development may be provided by flexible docking. Preliminary docking of inhibitors **8d** and **13** was performed using the crystal structure of rat farnesyltransferase (Figure 1). Subsequent homology modeling was performed with the enzyme inhibitor complex of inhibitor **13**. The overall topology of the active sites of rat/human and *P. falciparum* farnesyltransferases is quite similar with 72% sequence identity. The majority of amino acid side-chain changes from rat/human to *P. falciparum* are conservative in nature and should not affect the binding of the natural substrates significantly. However, when amino acid side chains engaged in inhibitor binding are analyzed, some important differences between the amino acid side chains contacting the inhibitor in the rat/human enzyme on one hand and in *P. falciparum* on the other hand can be noted (Figure 2): The binding site of inhibitor **13** consists of the enzyme's active site and an adjacent lipophilic region which accommodates the terminal phenylfuryl moiety, which we described previously as the far aryl binding site.[41] Here, the nitrophenylfuryl residue of inhibitor **13** is bound whereas the 2-acylaminobenzophenone core is harbored by the active site. Amino acid replacements concentrate on opposite sides of the inhibitor binding site affecting the binding of the nitrophenyl and the phenylacetyl moieties. In the far aryl binding site the replacements of Lys 356β by Asp, Gln 48β by Pro, and Thr 44β by Asn in *Pf*FTase probably do not affect the binding of the terminal biaryl moiety of inhibitor **13**. In contrast, the replacement of Glu 47β by Thr converts a hydrogen bond acceptor in the human enzyme to a moiety with hydrogen bond donor properties in the parasite FTase. This explains results obtained earlier, showing that substituents with hydrogen bond acceptor properties in this position yield farnesyltransferase inhibitors especially active against *P. falciparum*.[27] Therefore, it is of particular importance to have a hydrogen bond acceptor in the *para*-position of the terminal phenyl residue. In an earlier study,[27] using benzophenone derivatives without a basic function at the 2-acylamino moiety, we have shown that the nitro group can be replaced by other hydrogen bond acceptors (for example, a methylsulfonyl

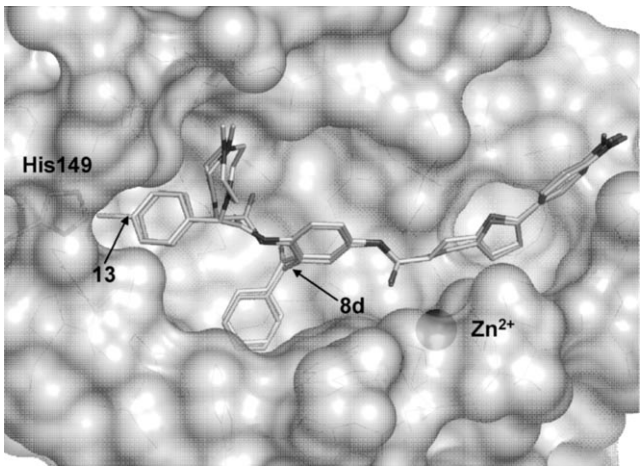

Figure 1. Superposition of docking results of the inhibitors **8d** (darker carbons) and **13** (brighter carbons) in the binding pocket of the farnesyltransferase. Only selective amino acids are shown. The zinc ion is indicated. Both inhibitors possess a similar binding mode. The slightly increased activity of compound **13** can be explained by an additional N-H···Cl interaction with His 149 (in part hidden by the surface).

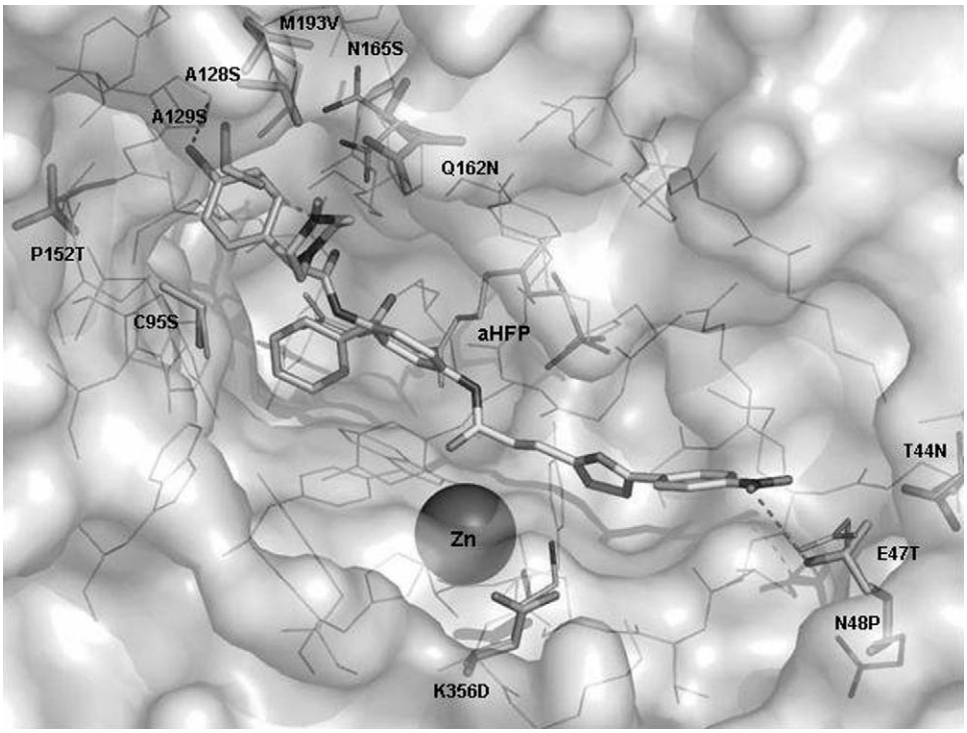

Figure 2. Homology model of *P. falciparum* farnesyltransferase (thicker residues) in comparison with rat/human farnesyltransferase (thinner residues). Differences in amino acids which might affect binding of inhibitor **13** are shown.

with this modification in the case of the α-piperazinyl derivative.

To overcome this effect and to obtain more active inhibitors, two approaches were envisioned. First, a methylene group was inserted between the α-position and the phenyl residue thereby obtaining α-piperazinyl-β-phenylpropionic acid derivative **18**. In docking studies, this compound behaved as expected, placing the piperazinyl moiety into the same region as the lead **13** and directing the terminal phenyl residue towards His 149β with a shorter distance to the imidazole residue because of the additional methylene group (Figure 3). However, the in vitro activity of inhibitor **18** did not improve as it was virtually equipotent to inhibitor **13** against blood stages of *P. falciparum* (Table 2). Furthermore, inhibitor **18** displayed higher cytotoxicity than **13**, resulting in a

moiety) what may be advantageous in terms of potential toxicity. Whether this also holds true for the types of inhibitors described herein will be addressed in separate studies. On the opposite side where the phenylpiperazinylacetic acid substructure is bound, amino acid changes from rat/human FTase to *Pf*FTase are more numerous. From these replacements, exchanges of Cys 95β to Ser, Pro 152β to Thr, and Ala 128α to Ser probably do not affect inhibitor binding significantly. However, replacement of Ala 129α by Ser provides a hydroxyl group capable of forming a hydrogen bond to N4 of the piperazinyl residue irrespective of its protonation state. Met 193β, Asn 165α, and Gln 162α are replaced by Val, Ser, and Asn, respectively, all amino acids with less spacious side chains. These exchanges probably also do not affect binding of inhibitor **13** but create some more space in the vicinity of the piperazinyl residue.

However, in spite of these differences between the structures of rat and *P. falciparum* farnesyltransferases the main clue derived from the docking studies with the rat structure remains valid. The chlorine substituent of the terminal phenyl is shown to be directed into a binding pocket pointing towards the imidazole residue of His 149β. Steric interference between the piperazinyl moiety and some amino acid side chains of the active site, however, prevents the chlorophenyl residue to be as deeply buried into this binding pocket as it is the case for the α-unsubstituted derivative. Thus, only a reduced interaction between the chlorine and the imidazole residue is possible, explaining the lower enhancement in activity associated

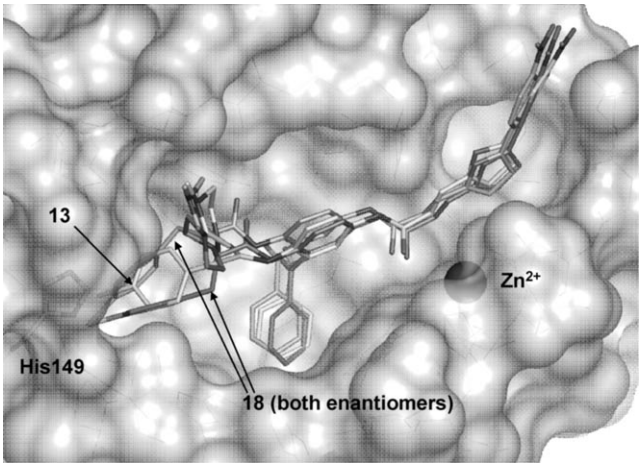

Figure 3. Docking of both enantiomers of inhibitor **18** into farnesyltransferase in comparison with inhibitor **13**. The docking yielded a binding mode for both enantiomers in which the additional methylene group facilitates a better chlorine His 149 interaction compared with **13**.

less favorable CC_{50}/IC_{50} ratio of 86. Therefore, this approach was discontinued.

A second strategy envisioned to overcome the steric hindrance by the piperazinyl moiety was the replacement of the piperazinyl moiety by an open chain ethylenediamine, expecting that the enhanced flexibility of this residue would allow for

both an optimal chlorine–imidazole interaction as well as for an interaction of the terminal amine with the amino acids in the upper part of the binding site. Indeed, when assayed in vitro against *P. falciparum* blood cultures the ethylenediamine derivatives **20** and **22** displayed considerably improved in vitro activity with IC_{50} values of 32 and 30 nM, respectively, thus being approximately sevenfold more active than inhibitor **13** (Table 3). An important feature is that the cytotoxicity of the para chloro-substituted derivatives **22** is significantly higher than that of the phenyl-unsubstituted derivative **20**. Although the absolute cytotoxicity of inhibitor **20** is higher than that of the lead **13** (CC_{50} values 14.4 and 38.6 μM, respectively), the CC_{50}/IC_{50} ratio is still considerably improved, with a value of 450, because of the significantly improved antimalarial activity of inhibitor **20**. Remarkably, the phenyl unsubstituted inhibitor **20** displayed a significantly higher activity in the mouse model (ED_{50} = 24 μmol (16 mg) kg^{-1} bw) than the para chloro substituted derivative **22** (ED_{50} = 37 μmol (26 mg)kg^{-1} bw). Furthermore, inhibitor **20** was also more active than the piperazinyl derivatives **8d** and **13**. The oral route has not been studied, however inhibitor **8f** has demonstrated oral activity in *T. cruzi* infected mice.[54]

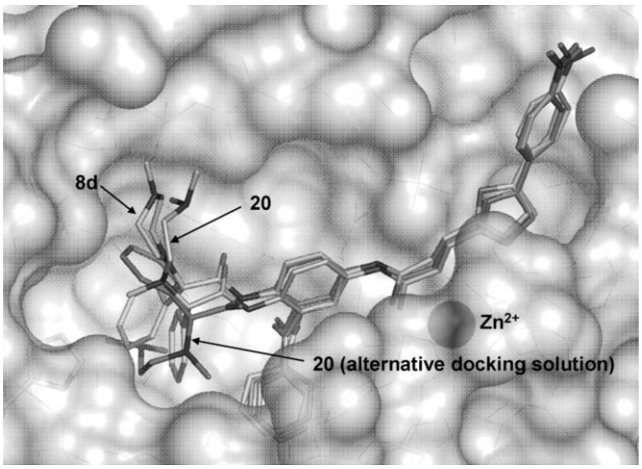

Figure 4. Superimposition of docking results of the methylpiperazinyl-substituted inhibitor **8d** and two different docking solutions of inhibitor **20**. In one docking solution an ethylene diamine residue points roughly into the same direction as the methylpiperazinyl moiety of inhibitor **8d**, whereas the phenyl residue is markedly shifted downwards, forming an edge to face interaction with Trp 102. In the second docking solution the phenyl and ethylene diamine moieties exchanged their positions.

The presumed binding mode of inhibitor **20** obtained with AutoDock3.0 varied considerably from the mode envisioned (Figure 4). In one mode the flexible ethylenediamine moiety was directed into the same region as the piperazinyl residue but the phenyl residue was not directed towards His 149β but was oriented more steeply downwards towards Trp 102β resembling a binding mode which we obtained earlier for simple α-amino acid derivatives.[42] In a second mode, the two residues at the α-carbon switched their positions with the aryl residue now being directed upwards into the region formerly occupied by the piperazinyl moiety and the ethylenediamine pointing towards His 149β. As energy values obtained for both solutions were virtually identical, no orientation can be favored at this time. Regardless which binding mode is realized in the enzyme, both binding modes are considerably different from the mode obtained for inhibitors **8d** and **13**, explaining the different effects of the introduction of a para chlorine into the terminal phenyl residue. Replacement of the ethylenediamine moiety by a trimethylenediamine resulted in a considerable reduction in in vitro activity with the para unsubstituted inhibitor **23** displaying an IC_{50} value of 100 nM and the para chloro substituted inhibitor **24** a value of 150 nM (Table 3). As with the ethylenediamine inhibitors, the chloro-substituted compound **24** showed a markedly higher cytotoxicity than the unsubstituted inhibitor **23**. Because of the in vitro results no in vivo experiments were undertaken. In contrast to the ethylenediamine derivatives only one binding mode was obtained from flexible

Table 3. Activity of open chain compounds **20** and **22–24**.

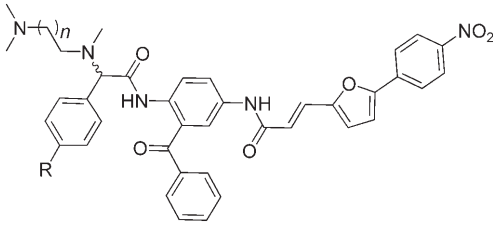

Compd	R	*n*	IC_{50} [nM] FTase	IC_{50} [nM] *P. falciparum*	ED_{50} [μmol kg^{-1}] (mg kg^{-1}) *P. vinckeii*	ED_{90} [μmol kg^{-1}] (mg kg^{-1}) *P. vinckeii*	CC_{50} [nM] HeLa	CC_{50}/IC_{50}
20	H	1	21 ± 3	32	24 [16]	30 [20]	14.4	450
22	Cl	1	28 ± 3	30	37 [26]	43 [30]	6.6	220
23	H	2	455 ± 111	100	nd[a]	nd	23.0	230
24	Cl	2	438 ± 69	150	nd	nd	8.9	60

[a] Not determined

docking. In this binding mode the trimethylenediamine moiety is pointing towards His 149β and the phenyl residue is pointing in an upward position, thus resembling one of the two binding modes obtained for the ethylenediamine derivatives. All attempts to obtain enantiomerically pure derivatives failed because of rapid racemization of the key intermediates.

Antiparasitic activity of the compounds does not only depend on the interactions with the FTase target protein but also on complex transport phenomena. Depending on the exact intracellular localization of their target, antimalarial drugs have to cross between three to seven membranes which properties are unfortunately not well understood yet. Physicochemical properties govern the access of a particular compound to its intracellular target as exemplified by numerous compounds which are highly active against the isolated target but more or less inactive against cultured parasites or in an animal model. Therefore, we also investigated the influence of ADME parameters. From altogether 45 parameters which were calculated (Supporting Information table 1) four parameters (Q_VSA_FPOL, Q_VSA_FHYD, log *S*, and Slog *P*; Supporting Information table 2) were selected and correlated with the negative logarithm of antiparasitic activity (Supporting Information figures 1–4). No clear linear correlation could be detected; the strongest one being the correlation with the fractional polar van der Waals surface area (Q_VSA_FPOL) ($R^2 = 0.4254$). Especially, the relative inactivity of the ethylpiperazine derivative **8e** in comparison with the methyl derivative **8d** and the propyl homologue **8f** cannot be explained on the basis of ADME parameters. A critical issue may be to explain the comparatively low enhancement in activity through the introduction of a chlorine into **8d** resulting in **13** and the considerable enhancement in activity when allowing higher conformational flexibility as in the ethylenediamine derivative **20**. Table 4 provides some selected molecular properties for these selected inhibitors and for the homologue 1,3-propyldiamine derivative **23** showing that a unified straight forward explanation SAR can still not be given on the basis of these parameters. In conclusion, we attribute the observed differences in antimalarial activity to a combination of effects of changes in physicochemical properties and activities against the presumed target farnesyltransferase.

Table 4. ADME (selected parameters for compounds **8d**, **13**, **20**, and **22**).

	ppfalc	IC_{50} [nM] *P. falciparum*	Q_VSA_FPOL	log *S*	Slog *P*
8d	6.57	270	0.33	−10.76	5.34
13	6.68	210	0.32	−11.49	6.00
20	7.49	32	0.34	−10.32	5.55
23	7.00	100	0.35	−10.61	5.59

Our inhibitors contain a biarylacrylic acid substructure which may act as a Michael acceptor, a structural feature normally unwanted in a potential drug. However, at this stage of development we are not particularly concerned about this because of the selective toxicity we have observed against cultured parasites in comparison with a human cell line and the apparent lack of toxicity of therapeutic doses in mice. Furthermore, such Michael acceptors are integral part of another class of antimalarials in preclinical development, the inhibitors of the digestive vacuole cysteine protease falcipain. In fact, we have some preliminary results indicating that some of our inhibitors have in addition to their effect on farnesyltransferase also some weak activity against falcipain. Having more than one mechanism of action is sometimes considered advantageous for a potential anti-infective agent.

Summary and Conclusion

Inhibition of farnesyltransferase from *P. falciparum* is a strategy for the development of novel antimalarials actively pursued in the last years. Several different structural classes of antimalarial farnesyltransferases are described.[47–51] Currently, tetrahydroquinolines represent the most advanced class of antimalarial farnesyltransferase inhibitors,[52,53] but given the imponderabilities of drug development, work on other lead structures should be continued.

Starting from benzophenone-based farnesyltransferase inhibitors with high in vitro antimalarial activity but no in vivo activity, the first farnesyltransferase inhibitors with in vivo antimalarial activity were obtained through the introduction of a methylpiperazinyl moiety into the α-position of the phenylacetic acid substructure.[28] Our homology modeling revealed some differences between the active sites of rat/human and *P. falciparum* farnesyltransferases, but the main clues derived from docking studies with the rat enzyme remain valid. Based on these docking results, in the following design cycle the piperazinyl moiety of our benzophenone-based inhibitors was replaced by a *N,N,N′*-trimethylethylenediamine moiety. This resulted in an inhibitor with significantly improved in vitro and in vivo antimalarial activity. Furthermore, this inhibitor displayed notable selectivity towards malaria parasites in comparison to human cells. This is a particularly important result for the development of specific antimalarial farnesyltransferase inhibitors.

Experimental Section

^{1}H NMR spectra were recorded on a Jeol Lambda 500 delta, a Jeol JNM-GX-400, a Jeol Eclipse 500 and a Jeol Eclipse 400 spectrometer. Mass spectra were obtained with a Vacuum Generator VG 7070 H using a Vector 1 data acquisition system from Teknivent, an AutoSpec mass spectrometer from Micromass, an API 2000 LC–MS–MS system of PE SCIEX using Analyst 1.2 of Applied Biosystems/MDS SCIEX and on a MStation JMS 700 from Jeol using Jeol Mass Data System MS–MP 9021D 2.30. IR spectra were recorded on a Nicolet 510P FTIR spectrometer and a Jasco FT/IR 410 FTIR spectrometer. Microanalyses were obtained with a CH analyzer according to Dr. Salzer from Labormatic, a Hewlett–Packard CHN analyzer type 185, and a Vario EL from Elementar. Melting points were obtained with a Reichert Austria microscope and are uncorrected. Column chromatography was carried out using silica gel 60 (0.062–0.200 mm) from Machery–Nagel and silica gel 60 (0.040–0.063) from Merck.

General procedure 1: Activation of various acids as acid chlorides and reaction with aromatic amines

The various carboxylic acids were dissolved in dichloromethane and 0.2 mL oxalylchloride per mmol acid was added. The mixture was stirred for 2 h and the volatiles were evaporated in vacuo. The resulting acyl chlorides were dissolved in dioxane (approximately 30 mL) and added to a solution of the appropriate aromatic amine in hot toluene (approximately 50 mL). The mixtures were heated under reflux for 2 h. Then, the solvent was removed in vacuo and the crude products were purified by recrystallization.

General procedure 2: Substitution of the halogen of 2-chloro- or 2-bromophenylalkylcarboxylic acid derivates with amines

The 2-halogene-phenylalkylcarboxylic acid derivative was dissolved in freshly distilled acetonitrile, 3 equivalents of the amine were added, and the mixture was heated under reflux for 24–48 h. After removing the acetonitrile under reduced pressure, the obtained solid was dissolved in ethyl acetate and was purified either by column chromatography or by washing with a saturated solution of K_2CO_3, drying over Na_2SO_4, and removing the solvent under reduced pressure. In case further purification was necessary, the crude product was recrystallized or subject to chromatography on silica gel.

General procedure 3: Reduction of aromatic nitro compounds

Aromatic nitro compounds were dissolved in ethyl acetate (50–100 mL) and $SnCl_2{\cdot}2H_2O$ (1.125 g per mmol nitro compound) was added. The mixture was heated under reflux for 2 h. Then, $NaHCO_3$ solution was added until pH 7–8 was reached and the organic layer was separated. The aqueous layer was extracted three times with ethyl acetate. The combined organic layers were washed with brine and dried over $MgSO_4$. Then, the solvent was removed in vacuo to obtain the crude products.

General procedure 4: Bromination of carboxylic acids

The carboxylic acid, bromine (1.05 mmol per mmol carboxylic acid) and phosphortrichloride (0.12 mmol per mmol carboxylic acid) were dissolved in 40 mL benzene. The solution was heated under reflux carefully for 2–3 days until the dark color of the bromine disappeared. Then, the benzene was evaporated under reduced pressure to give an oily product, which was dissolved in *n*-hexane under heating. Then, the mixture was stored at $-25\,^{\circ}C$ for 24 h to obtain the crude product.

(*R*,*S*)-*N*-(2-Benzoyl-4-nitrophenyl)-2-chloro-2-phenylacetamide (5). According to general procedure 1 from (*R*,*S*)-2-chloro-2-phenylacetylchloride (0.73 mL, 5.0 mmol) and 2-amino-5-nitrobenzophenone (1211 mg, 5.0 mmol). Purification: recrystallization from ethanol to give a yellow solid: yield 1793 mg (91%). ^{1}H NMR (500 MHz, $CDCl_3$): $\delta = 5.50$ (s, 1H), 7.34–7.45 (m, 3H), 7.53–7.57 (m, 4H), 7.66–7.74 (m, 3H), 8.39–8.50 (m, 2H), 8.86–8.88 (m, 1H), 12.09 ppm (s, 1H).

(*R*,*S*)-*N*-(2-Benzoyl-4-nitrophenyl)-2-phenyl-2-(1-piperidinyl)acetamide (6a). According to general procedure 2 from (*R*,*S*)-*N*-(2-benzoyl-4-nitrophenyl)-2-chloro-2-phenylacetamide (1580 mg, 4.0 mmol) and piperidine (1.0 mL, 12.0 mmol). Purification: recrystallization from ether/*n*-hexane (1:1) to give a yellow solid: yield 646 mg (35%). ^{1}H NMR (500 MHz, [D$_6$]DMSO): $\delta = 1.29$ (m, 2H), 1.48 (m, 4H), 2.23 (m, 4H), 4.11 (s, 1H), 7.23–7.35 (m, 5H), 7.54–7.79 (m, 5H), 8.23–8.51 (m, 3H), 11.50 ppm (s, 1H).

(*R*,*S*)-*N*-(4-Amino-2-benzoylphenyl)-2-phenyl-2-(1-piperidinyl)acetamide (7a). According to general procedure 3 from (*R*,*S*)-*N*-(2-benzoyl-4-nitrophenyl)-2-phenyl-2-(1-piperidinyl)acetamide (532 mg, 1.2 mmol) and tin(II) chloride dihydrate (1.35 g, 6.0 mmol). Red solid: yield 491 mg (92%). ^{1}H NMR (500 MHz, [D$_6$]DMSO): $\delta =$ 1.45 (m, 6H), 1.90 (m, 4H), 3.85 (s, 1H), 5.19 (s, 2H), 6.73–6.81 (m, 2H), 7.23–7.75 (m, 11H), 10.55 ppm (s, 1H).

(*E*)-(*R*,*S*)-*N*-{3-Benzoyl-4-[2-phenyl-2-(1-piperidinyl)acetylamino]-phenyl}-3-[5-(4-nitrophenyl)-2-furyl]acrylic acid amide (8a). According to general procedure 1 from (*E*)-3-[5-(4-nitrophenyl)-2-furyl]-acrylic acid chloride (195 mg, 0.75 mmol) and (*R*,*S*)-*N*-(4-amino-2-benzoylphenyl)-2-phenyl-2-(1-piperidinyl)acetamide (310 mg, 0.75 mmol). Purification: recrystallization from toluene/dioxane (1:1) to give a yellow solid: yield 131 mg (27%); mp 195 °C; IR (KBr): $\tilde{\nu} = 3408$, 2956, 1700, 1697, 1666, 1653, 1623, 1598, 1560, 1513, 1453, 1404, 1333, 1251, 1199, 1181, 1109, 871, 853, 753, 697 cm^{-1}; ^{1}H NMR (500 MHz, [D$_6$]DMSO): $\delta = 1.62$ (m, 6H), 3.55 (m, 4H), 5.15 (s, 1H), 6.79 (d, $J = 16$ Hz, 1H), 7.04–7.05 (m, 1H), 7.27–7.29 (m, 2H), 7.39 (d, $J = 16$ Hz, 1H), 7.44–7.65 (m, 8H), 7.78–8.00 (m, 6H), 8.31–8.33 (m, 2H), 10.63 (s, 1H), 11.37 ppm (s, 1H); MS (ESI): *m/z* 655 (100, $[M+H]^+$), 472 (1), 456 (11), 442 (1), 405 (4), 174 (5). Anal. ($C_{39}H_{34}N_4O_6$) C, H, N.

(*R*,*S*)-*N*-(2-Benzoyl-4-nitrophenyl)-2-(4-oxo-1-piperidinyl)-2-phenylacetamide (6b). According to general procedure 2 from (*R*,*S*)-*N*-(2-benzoyl-4-nitrophenyl)-2-chloro-2-phenylacetamide (1580 mg, 4.0 mmol), 4-piperidone hydrochloride·H$_2$O (2873 mg, 18.0 mmol), $NaHCO_3$ (1512 mg, 18.0 mmol), and molecular sieve. Purification: chromatography on silica gel (ethyl acetate) to give a yellow solid: yield 1464 mg (53%). ^{1}H NMR (500 MHz, $CDCl_3$): $\delta = 2.60$ (m, 4H,), 2.72 (m, 2H), 2.82 (m, 2H), 4.25 (s, 1H), 7.34–7.41 (m, 5H), 7.55–7.77 (m, 5H), 8.38–8.43 (m, 2H), 8.49–8.50 (m, 1H), 12.48 ppm (s, 1H).

(*R*,*S*)-*N*-(4-Amino-2-benzoylphenyl)-2-(4-oxo-1-piperidinyl)-2-phenylacetamide (7b). According to general procedure 3 from (*R*,*S*)-*N*-(2-benzoyl-4-nitrophenyl)-2-(4-oxo-1-piperidinyl)-2-phenylacetamide (1418 mg, 3.1 mmol) and tin(II)-chloride-dihydrate (3.49 g, 15.5 mmol). Yellow-orange solid: yield 1197 mg (90%). ^{1}H NMR (500 MHz, $CDCl_3$): $\delta = 1.76$ (m, 4H), 2.36 (m, 4H), 3.54 (s, 2H), 3.82 (s, 1H), 6.70–6.77 (m, 2H), 7.17–7.27 (m, 3H), 7.30–7.35 (m, 2H), 7.39–7.44 (m, 2H), 7.51–7.55 (m, 1H), 7.61–7.72 (m, 2H), 8.17–8.21 (m, 1H), 11.15 ppm (s, 1H).

(*E*)-(*R*,*S*)-*N*-{3-Benzoyl-4-[2-(4-oxo-1-piperidinyl)-2-phenylacetylamino]phenyl}-3-[5-(4-nitrophenyl)-2-furyl]acrylic acid amide (8b). According to general procedure 1 from (*E*)-3-[5-(4-nitrophenyl)-2-furyl]acrylic acid chloride (286 mg, 1.1 mmol) and (*R*,*S*)-*N*-(4-amino-2-benzoylphenyl)-2-(4-oxo-1-piperidinyl)-2-phenylacetamide (470 mg, 1.1 mmol). Yellow solid: yield 359 mg (49%); mp 181 °C; IR (KBr): $\tilde{\nu} = 3426$, 2924, 1733, 1695, 1653, 1623, 1597, 1559, 1539, 1516, 1457, 1404, 1332, 1293, 1246, 1180, 1027, 970, 852, 753 cm^{-1}; ^{1}H NMR (500 MHz, [D$_6$]DMSO): $\delta = 2.48$ (s, 4H), 3.51 (s, 4H), 5.35 (s, 1H), 6.81 (d, $J = 16$ Hz, 1H), 7.12–7.14 (m, 1H), 7.38–7.57 (m, 8H and d, $J = 16$ Hz, 1H), 7.61–7.66 (m, 1H), 7.72–7.78 (m, 3H), 7.83–8.05 (m, 3H), 8.31–8.33 (m, 2H), 8.90–8.91 (m, 1H), 10.69 (s, 1H), 11.50 ppm (s, 1H); MS (FAB): *m/z* 669 (9, $[M+H]^+$), 581 (20), 528 (11), 428 (20), 354 (8), 242 (3). Anal. ($C_{39}H_{32}N_4O_7$) C, H, N.

(*R*,*S*)-*N*-(2-Benzoyl-4-nitrophenyl)-2-(4-morpholinyl)-2-phenylacetamide (6c). According to general procedure 2 from (*R*,*S*)-*N*-(2-benzoyl-4-nitrophenyl)-2-chloro-2-phenylacetamide (1580 mg,

4.0 mmol) and morpholine (1.04 mL, 12.0 mmol). Purification: recrystallization from ethyl acetate to give a white solid: yield 1055 mg (58%). ^{1}H NMR (500 MHz, [D$_6$]DMSO): $\delta = 2.49$ (s, 4H), 3.60 (s, 4H), 4.14 (s, 1H), 7.31–7.33 (m, 5H), 7.56–7.82 (m, 5H), 8.26–8.47 (m, 3H), 11.67 ppm (s, 1H).

(*R*,*S*)-*N*-(4-Amino-2-benzoylphenyl)-2-(4-morpholinyl)-2-phenylacetamide (7c). According to general procedure 3 from (*R*,*S*)-*N*-(2-benzoyl-4-nitrophenyl)-2-(4-morpholinyl)-2-phenylacetamide (668 mg, 1.5 mmol) and tin(II)-chloride-dihydrate (1.69 g, 7.5 mmol). Yellow solid: yield 600 mg (93%). ^{1}H NMR (500 MHz, [D$_6$]DMSO): $\delta = 2.17$ (s, 4H), 3.53 (s, 4H), 3.84 (s, 1H), 5.20 (s, 2H), 6.63–6.72 (m, 2H), 7.27–7.31 (m, 5H), 7.52–7.72 (m, 6H), 10.49 ppm (s, 1H).

(*E*)-(*R*,*S*)-*N*-{3-Benzoyl-4-[2-(4-morpholinyl)-2-phenylacetylamino]-phenyl}-3-[5-(4-nitrophenyl)-2-furyl]acrylic acid amide (8c). According to general procedure 1 from (*E*)-3-[5-(4-nitrophenyl)-2-furyl]acrylic acid chloride (195 mg, 0.75 mmol) and (*R*,*S*)-*N*-(4-amino-2-benzoylphenyl)-2-(4-morpholinyl)-2-phenylacetamide (321 mg, 0.75 mmol). Purification: washing with saturated $NaHCO_3$ solution and recrystallization from ethanol to give a red-orange solid: yield 305 mg (62%); mp 255 °C; IR (KBr): $\tilde{\nu} = 3444$, 2959, 1660, 1627, 1598, 1511, 1404, 1334, 1289, 1248, 1111, 854, 753, 703 cm^{-1}; ^{1}H NMR (500 MHz, [D$_6$]DMSO): $\delta = 2.49$ (s, 4H), 3.58 (s, 4H), 3.97 (s, 1H), 6.73 (d, $J = 16$ Hz, 1H), 7.02–7.03 (m, 1H), 7.29–7.24 (m, 6H and d, $J = 16$ Hz, 1H), 7.55–7.90 (m, 7H), 7.97–8.05 (m, 3H), 8.30–8.32 (m, 2H), 10.45 (s, 1H), 11.08 ppm (s, 1H); MS (ESI): *m/z* 657 (100, $[M+H]^+$), 528 (2), 416 (6), 333 (4), 298 (16), 271 (6), 185 (2), 130 (4), 121 (4). Anal. ($C_{38}H_{32}N_4O_7$) C, H, N.

(*R*,*S*)-*N*-(2-Benzoyl-4-nitrophenyl)-2-(4-methyl-1-piperazinyl)-2-phenylacetamide (6d). According to general procedure 2 from (*R*,*S*)-*N*-(2-benzoyl-4-nitrophenyl)-2-chloro-2-phenylacetamide (945 mg, 2.4 mmol) and *N*-methylpiperazine (0.80 mL, 7.2 mmol). Purification: recrystallization from ethanol to give a yellow solid: yield 693 mg (63%). ^{1}H NMR (500 MHz, $CDCl_3$): $\delta = 2.26$ (s, 3H), 2.53 (s, 8H), 4.01 (s, 1H), 7.29 (m, 3H), 7.35 (m, 2H), 7.55 (m, 2H), 7.68 (m, 1H), 7.77 (m, 2H), 8.34 (m, 1H), 8.43 (m, 1H), 8.85 (m, 1H), 12.09 ppm (s, 1H).

(*R*,*S*)-*N*-(4-Amino-2-benzoylphenyl)-2-(4-methyl-1-piperazinyl)-2-phenylacetamide (7d). According to general procedure 3 from (*R*,*S*)-*N*-(2-benzoyl-4-nitrophenyl)-2-(4-methyl-1-piperazinyl)-2-phenylacetamide (553 mg, 1.2 mmol) and tin(II)-chloride-dihydrate (1.35 g, 6.0 mmol). Red oil: yield 439 mg (85%). ^{1}H NMR (400 MHz, $CDCl_3$): $\delta = 2.00$ (s, 8H). 2.65 (s, 3H), 3.98 (s, 1H), 6.75 (m, 1H), 6.82 (m, 1H), 7.24 (m, 3H), 7.29 (m, 2H), 7.45 (m, 2H), 7.56 (m, 1H), 7.67 (m, 1H), 8.26 (m, 1H), 11.39 ppm (s, 1H).

(*E*)-(*R*,*S*)-*N*-{3-Benzoyl-4-[2-(4-methyl-1-piperazinyl)-2-phenylacetylamino]phenyl}-3-[5-(4-nitrophenyl)-2-furyl]acrylic acid amide (8d). According to general procedure 1 from (*E*)-3-[5-(4-nitrophenyl)-2-furyl]acrylic acid chloride (260 mg, 1.0 mmol) and (*R*,*S*)-*N*-(4-amino-2-benzoylphenyl)-2-(4-ethyl-1-piperazinyl)-2-phenylacetamide (428 mg, 1.0 mmol). Purification: recrystallization from toluene to give a red solid: yield 152 mg (23%); mp 160 °C; IR (KBr): $\tilde{\nu} = 3426$, 1682, 1630, 1598, 1547, 1510, 1402, 1332, 1286, 1225, 1153, 1112, 1072, 979, 852, 752, 695 cm^{-1}; ^{1}H NMR (400 MHz, [D$_6$]DMSO): $\delta = 2.28$ (s, 8H), 2.71 (s, 3H), 4.19 (s, 1H), 6.79 (d, $J =$ 16 Hz, 1H), 7.02 (m, 1H), 7.14 (m, 2H), 7.23 (m, 4H), 7.32 (m, 4H), 7.40 (m, 2H), 7.55 (m, 2H), 7.76 (m, 2H), 7.99 (m, 2H), 8.31 (m, 2H), 10.51 (s, 1H), 10.88 ppm (s, 1H), MS (EI): *m/z* 428 (2), 212 (3), 190 (15), 189 (100), 105 (8), 91 (7), 77 (4), 70 (3). Anal. ($C_{39}H_{35}N_5O_6$) C, H, N.

(*R*,*S*)-*N*-(2-Benzoyl-4-nitrophenyl)-2-(4-ethyl-1-piperazinyl)-2-phenylacetamide (6e). According to general procedure 2 from (*R*,*S*)-*N*-(2-benzoyl-4-nitrophenyl)-2-chloro-2-phenylacetamide (2367 mg, 6.0 mmol) and *N*-ethylpiperazine (2.3 mL, 18.0 mmol). Purification: chromatography on silica gel (ethyl acetate) to give a yellow oil: yield 850 mg (30%). ^{1}H NMR (500 MHz, $CDCl_3$): $\delta = 1.17$ (t, $J = 8$ Hz, 3H), 2.00 (m, 2H), 2.89 (s, 4H), 3.16 (s, 4H), 4.68 (s, 1H), 7.30–7.43 (m, 5H), 7.52–7.87 (m, 5H), 8.38–8.49 (m, 2H), 8.86–8.89 (m, 1H), 12.25 ppm (s, 1H).

(*R*,*S*)-*N*-(4-Amino-2-benzoylphenyl)-2-(4-ethyl-1-piperazinyl)-2-phenylacetamide (7e). According to general procedure 3 from (*R*,*S*)-*N*-(2-benzoyl-4-nitrophenyl)-2-(4-ethyl-1-piperazinyl)-2-phenylacetamide (756 mg, 1.6 mmol) and tin(II)-chloride-dihydrate (1.8 g, 8.0 mmol). Brown solid: yield 569 mg (80%). ^{1}H NMR (400 MHz, $CDCl_3$): $\delta = 1.11$ (t, $J = 8$ Hz, 1H), 2.20 (m, 2H), 2.60 (s, 8H), 3.94 (s, 1H), 4.48 (s, 2H), 6.85–7.23 (m, 5H), 7.25–7.41 (m, 5H), 7.48–7.52 (m, 2H), 7.77–7.79 (m, 1H), 11.24 ppm (s, 1H).

(*E*)-(*R*,*S*)-*N*-{3-Benzoyl-4-[2-(4-ethyl-1-piperazinyl)-2-phenylacetylamino]phenyl}-3-[5-(4-nitrophenyl)-2-furyl]acrylic acid amide (8e). According to general procedure 1 from (*E*)-3-[5-(4-nitrophenyl)-2-furyl]acrylic acid chloride (260 mg, 1.0 mmol) and (*R*,*S*)-*N*-(4-amino-2-benzoylphenyl)-2-(4-ethyl-1-piperazinyl)-2-phenylacetamide (443 mg, 1.0 mmol). Yellow solid: yield 438 mg (64%); mp 168 °C; IR (KBr): $\tilde{\nu} = 3409$, 2979, 1698, 1597, 1495, 1448, 1409, 1337, 1296, 1181, 1119, 1078, 1019, 872, 851, 736, 699, 653 cm^{-1}; ^{1}H NMR (400 MHz, [D$_6$]DMSO): $\delta = 1.18$ (t, $J = 8$ Hz, 3H), 2.27 (m, 2H), 3.03 (m, 4H), 3.27 (m, 4H), 4.68 (s, 1H), 7.05 (d, $J = 16$ Hz, 1H), 7.11–7.37 (m, 12H and d, $J = 16$ Hz, 1H), 7.52–7.78 (m, 7H), 10.96 (s, 1H), 11.10 ppm (s, 1H); MS (ESI): *m/z* 684 (100, $[M+H]^+$), 565 (3), 543 (100), 520 (3), 498 (21), 485 (7), 413 (3), 384 (11), 368 (21), 280 (21), 250 (3), 203 (44), 175 (3), 101 (4). Anal. ($C_{40}H_{37}N_5O_6$) C, H, N.

(*R*,*S*)-*N*-(2-Benzoyl-4-nitrophenyl)-2-phenyl-2-(4-propyl-1-piperazinyl)acetamide (6f). According to general procedure 2 from (*R*,*S*)-*N*-(2-benzoyl-4-nitrophenyl)-2-chloro-2-phenylacetamide (2367 mg, 6.0 mmol), *N*-propylpiperazine dihydrobromide (5221 mg, 18.0 mmol), $NaHCO_3$ (3024 mg, 36.0 mmol) and molecular sieve. Purification: chromatography on silica gel (1. ethyl acetate, 2. ethanol) to give a yellow oil: yield 1300 mg (45%). ^{1}H NMR (500 MHz, $CDCl_3$): $\delta = 0.94$ (t, $J = 8$ Hz, 3H), 1.67 (m, 2H), 2.00 (s, 8H), 2.79 (m, 2H), 4.11 (s, 1H), 7.34–7.36 (m, 5H), 7.58–7.60 (m, 2H), 7.74–7.78 (m, 3H), 8.40–8.48 (m, 2H), 8.87–8.89 (m, 1H), 12.24 ppm (s, 1H).

(*R*,*S*)-*N*-(4-Amino-2-benzoylphenyl)-2-phenyl-2-(4-propyl-1-piperazinyl)acetamide (7f). According to general procedure 3 from (*R*,*S*)-*N*-(2-benzoyl-4-nitrophenyl)-2-phenyl-2-(4-propyl-1-piperazinyl)acetamide (1265 mg, 2.6 mmol) and tin(II)-chloride-dihydrate (2.93 g, 13.0 mmol). Orange solid: yield 979 mg (82%). ^{1}H NMR (400 MHz, $CDCl_3$): $\delta = 0.92$ (t, $J = 8$ Hz, 1H), 1.67 (m, 2H), 2.03 (s, 8H), 2.79 (m, 2H), 3.20 (s, 2H), 4.09 (s, 1H), 6.79–6.86 (m, 2H), 7.25–7.73 (m, 10H), 8.20–8.30 (m, 1H), 11.40 ppm (s, 1H).

(*E*)-(*R*,*S*)-*N*-{3-Benzoyl-4-[2-phenyl-2-(4-propyl-1-piperazinyl)acetylamino]phenyl}-3-[5-(4-nitrophenyl)-2-furyl]acrylic acid amide (8f). According to general procedure 1 from (*E*)-3-[5-(4-nitrophenyl)-2-furyl]acrylic acid chloride (260 mg, 1.0 mmol) and (*R*,*S*)-*N*-(4-amino-2-benzoylphenyl)-2-phenyl-2-(4-propyl-1-piperazinyl)acetamide (456 mg, 1.0 mmol). Yellow solid: yield 223 mg (32%); mp 173 °C; IR (KBr): $\tilde{\nu} = 3420$, 2967, 1697, 1596, 1515, 1448, 1403, 1332, 1295, 1252, 1180, 698 cm^{-1}; ^{1}H NMR (400 MHz, [D$_6$]DMSO): $\delta = 0.84$ (t, $J = 8$ Hz, 3H), 1.69 (m, 2H), 2.99 (s, 4H), 3.01 (s, 4H), 3.40 (m, 2H), 4.62 (s, 1H), 6.83 (d, $J = 16$ Hz, 1H), 7.36–7.53 (m, 10H and d, $J = 16$ Hz, 1H), 7.62–7.81 (m, 8H), 8.31–9.33 (m, 1H), 11.13 (s, 1H),

11.24 ppm (s, 1H); MS (ESI): *m/z* 698 (83, $[M+H]^+$), 557 (91), 543 (17), 512 (100), 499 (49). Anal. ($C_{41}H_{39}N_5O_6$) C, H, N.

(*R*,*S*)-*N*-(2-Benzoyl-4-nitrophenyl)-2-[4-(2-hydroxyethyl)-1-piperazinyl]-2-phenylacetamide (6g). According to general procedure 2 from (*R*,*S*)-*N*-(2-benzoyl-4-nitrophenyl)-2-chloro-2-phenylacetamide (2367 mg, 6.0 mmol), *N*-2-(hydroxyethyl)piperazine (2343 mg, 18.0 mmol). Purification: chromatography on silica gel (ethyl acetate) to give a white solid: yield 303 mg (10%). ^{1}H NMR (500 MHz, $CDCl_3$): $\delta = 2.57$ (s, 8H), 2.64 (m, 2H), 3.58 (m, 2H), 4.06 (s, 1H), 7.26–7.40 (m, 5H), 7.47–7.85 (m, 5H), 8.36–8.46 (m, 2H), 8.87–8.89 (m, 1H), 12.15 ppm (s, 1H).

(*R*,*S*)-*N*-(4-Amino-2-benzoylphenyl)-2-[4-(2-hydroxyethyl)-1-piperazinyl]-2-phenylacetamide (7g). According to general procedure 3 from (*R*,*S*)-*N*-(2-benzoyl-4-nitrophenyl)-2-[4-(2-hydroxyethyl)-1-piperazinyl]-2-phenylacetamide (293 mg, 0.6 mmol) and tin(II)-chloride-dihydrate (0.68 g, 3.0 mmol). Yellow solid: yield 261 mg (95%). ^{1}H NMR (400 MHz, $CDCl_3$): $\delta = 2.57$ (m, 2H), 2.63 (s, 8H), 3.34 (s, 2H), 3.58 (m, 2H), 3.92 (s, 1H), 6.78–6.86 (m, 2H), 7.25–7.62 (m, 8H), 7.77–7.79 (m, 2H), 8.26–8.28 (m, 1H), 11.21 ppm (s, 1H).

(*E*)-(*R*,*S*)-*N*-(3-Benzoyl-4-{2-[4-(2-hydroxyethyl)-1-piperazinyl]-2-phenylacetylamino}phenyl)-3-[5-(4-nitrophenyl)-2-furyl]acrylic acid amide (8g). According to general procedure 1 from (*E*)-3-[5-(4-nitrophenyl)-2-furyl]acrylic acid chloride (130 mg, 0.5 mmol) and (*R*,*S*)-*N*-(4-amino-2-benzoylphenyl)-2-[4-(2-hydroxyethyl)-1-piperazinyl]-2-phenylacetamide (230 mg, 0.5 mmol). Yellow solid: yield 295 mg (84%); mp 172 °C; IR (KBr): $\tilde{\nu} = 3377$, 2958, 1695, 1627, 1597, 1513, 1448, 1405, 1333, 1293, 1253, 1181, 1117, 1081, 872, 852, 734, 697 cm^{-1}; ^{1}H NMR (500 MHz, [D$_6$]DMSO): $\delta = 2.78$ (m, 2H), 3.58 (s, 8H), 3.81 (m, 2H), 4.59 (s, 1H), 6.86 (d, $J = 16$ Hz, 1H), 7.34–7.83 (m, 14H and d, $J = 16$ Hz, 1H), 7.97–8.05 (m, 3H), 8.33–8.39 (m, 2H), 10.69 (s, 1H), 11.04 ppm (s, 1H); MS (ESI): *m/z* 700 (48, $[M+H]^+$), 581 (9), 559 (100), 500 (4), 425 (4), 241 (5), 219 (34), 175 (4), 139 (5), 101 (26). Anal. ($C_{40}H_{37}N_5O_7$) C, H, N.

(*R*,*S*)-*N*-(2-Benzoyl-4-nitrophenyl)-2-[4-(*N*-isopropylaminocarbonylmethyl)-1-piperazinyl]-2-phenylacetamide (6h). According to general procedure 2 from (*R*,*S*)-*N*-(2-benzoyl-4-nitrophenyl)-2-chloro-2-phenylacetamide (2367 mg, 6.0 mmol), *N*-isopropyl-1-piperazineacetamide (3335 mg, 18.0 mmol). Purification: chromatography on silica gel (ethyl acetate) to give a yellow solid: yield 1936 mg (59%). ^{1}H NMR (500 MHz, $CDCl_3$): $\delta = 1.13$ (m, 6H), 2.64 (s, 8H), 2.96 (s, 2H), 4.07 (s, 1H), 4.11 (m, 1H), 6.83 (s, 1H), 7.28–7.44 (m, 5H), 7.58–7.86 (m, 5H), 8.36–8.47 (m, 2H), 8.86–8.89 (m, 1H), 12.18 ppm (s, 1H).

(*R*,*S*)-*N*-(4-Amino-2-benzoylphenyl)-2-[4-(*N*-isopropylaminocarbonylmethyl)-1-piperazinyl]-2-phenylacetamide (7h). According to general procedure 3 from (*R*,*S*)-*N*-(2-benzoyl-4-nitrophenyl)-2-[4-(*N*-isopropylaminocarbonylmethyl)-1-piperazinyl]-2-phenylacetamide (1903 mg, 3.5 mmol) and tin(II)-chloride-dihydrate (3.94 g, 17.5 mmol). Yellow solid: yield 1237 mg (69%). ^{1}H NMR (500 MHz, $CDCl_3$): $\delta = 1.09$ (m, 6H), 2.58 (s, 4H), 2.60 (s, 4H), 2.99 (s, 2H), 3.62 (s, 2H), 3.93 (s, 1H), 4.05 (m, 1H), 6.80 (s, 1H), 6.84–6.86 (m, 2H), 7.26–7.63 (m, 8H), 7.77–7.79 (m, 2H), 8.26–8.28 (m, 1H), 11.23 ppm (s, 1H).

(*E*)-(*R*,*S*)-*N*-(3-Benzoyl-4-{2-[4-(*N*-isopropylaminocarbonylmethyl)-1-piperazinyl]-2-phenylacetylamino}phenyl)-3-[5-(4-nitrophenyl)-2-furyl]acrylic acid amide (8h). According to general procedure 1 from (*E*)-3-[5-(4-nitrophenyl)-2-furyl]acrylic acid chloride (260 mg, 1.0 mmol) and (*R*,*S*)-*N*-(4-amino-2-benzoylphenyl)-2-[4-(*N*-isopropylaminocarbonylmethyl)-1-piperazinyl]-2-phenylacetamide (514 mg, 1.0 mmol). Yellow solid: yield 412 mg (55%); mp 180 °C; IR (KBr): $\tilde{\nu} = 3434$, 2971, 1678, 1624, 1597, 1551, 1514, 1449, 1403, 1332, 1292, 1249, 1178, 852, 697 cm^{-1}; ^{1}H NMR (500 MHz, [D$_6$]DMSO): $\delta =$ 1.07 (m, 6H), 2.71 (s, 2H), 3.55 (s, 4H), 3.85 (s, 4H), 4.27 (m, 1H), 4.48 (s, 1H), 6.80 (d, $J = 16$ Hz, 1H), 7.04 (s, 1H), 7.36–7.77 (m, 12H and d, $J = 16$ Hz, 1H), 7.80–8.01 (m, 4H), 8.31–8.33 (m, 2H), 8.57–8.59 (m, 1H), 10.67 (s, 1H), 10.99 ppm (s, 1H); MS (ESI): *m/z* 755 (100, $[M+H]^+$), 615 (54), 337 (38), 316 (47), 241 (26), 217 (11), 185 (14). Anal. ($C_{43}H_{42}N_6O_7$) C, H, N.

(*R*,*S*)-*N*-(2-Benzoyl-4-nitrophenyl)-2-(4-cyclohexyl-1-piperazinyl)-2-phenylacetamide (6i). According to general procedure 2 from (*R*,*S*)-*N*-(2-benzoyl-4-nitrophenyl)-2-chloro-2-phenylacetamide (2367 mg, 6.0 mmol), *N*-cyclohexylpiperazine (3029 mg, 18.0 mmol). Purification: chromatography on silica gel (ethyl acetate) to give a yellow solid: yield 965 mg (31%). ^{1}H NMR (500 MHz, $CDCl_3$): $\delta =$ 1.27 (m, 6H), 1.78 (m, 4H), 2.22 (m, 1H), 2.55 (s, 8H), 4.04 (s, 1H), 7.35–7.43 (m, 5H), 7.56–7.82 (m, 5H), 8.36–8.45 (m, 2H), 8.86–8.88 (m, 1H), 12.10 ppm (s, 1H).

(*R*,*S*)-*N*-(4-Amino-2-benzoylphenyl)-2-(4-cyclohexyl-1-piperazinyl)-2-phenylacetamide (7i). According to general procedure 3 from (*R*,*S*)-*N*-(2-benzoyl-4-nitrophenyl)-2-(4-cyclohexyl-1-piperazinyl)-2-phenylacetamide (948 mg, 1.8 mmol) and tin(II)-chloride-dihydrate (2.03 g, 9.0 mmol). Yellow solid: yield 791 mg (88%). ^{1}H NMR (500 MHz, $CDCl_3$): $\delta = 1.26$ (m, 6H), 1.85 (m, 4H), 2.29 (m, 1H), 2.62 (s, 8H), 3.55 (s, 2H), 3.91 (s, 1H), 7.17–7.54 (m, 10H), 7.80–7.81 (m, 2H), 8.25–8.26 (m, 1H), 11.12 ppm (s, 1H).

(*E*)-(*R*,*S*)-*N*-{3-Benzoyl-4-[2-(4-cyclohexyl-1-piperazinyl)-2-phenylacetylamino]phenyl}-3-[5-(4-nitrophenyl)-2-furyl]acrylic acid amide (8i). According to general procedure 1 from (*E*)-3-[5-(4-nitrophenyl)-2-furyl]acrylic acid chloride (260 mg, 1.0 mmol) and (*R*,*S*)-*N*-(4-amino-2-benzoylphenyl)-2-(4-cyclohexyl-1-piperazinyl)-2-phenylacetamide (497 mg, 1.0 mmol). Yellow solid: yield 211 mg (29%); mp 189 °C; IR (KBr): $\tilde{\nu} = 3420$, 2938, 2857, 1693, 1625, 1598, 1514, 1449, 1404, 1333, 1290, 1252, 1182, 1109, 1026, 971, 940, 872, 852, 753, 697, 651 cm^{-1}; ^{1}H NMR (500 MHz, [D$_6$]DMSO): $\delta =$ 1.27 (m, 6H), 1.80 (m, 4H), 2.28 (s, 1H), 3.20 (s, 4H), 3.50 (s, 4H), 4.45 (s, 1H), 6.79 (d, $J = 16$ Hz, 1H), 7.04–7.05 (m, 1H), 7.37–7.55 (m, 9H and d, $J = 16$ Hz, 1H), 7.66–7.77 (m, 4H), 7.91–8.01 (m, 3H), 8.31–8.34 (m, 2H), 10.65 (s, 1H), 10.99 ppm (s, 1H); MS (ESI): *m/z* 738 (100, $[M+H]^+$), 597 (60), 273 (11), 257 (6), 175 (5), 101 (5). Anal. ($C_{44}H_{43}N_5O_6$) C, H, N.

(*R*,*S*)-*N*-(2-Benzoyl-4-nitrophenyl)-2-(4-phenyl-1-piperazinyl)-2-phenylacetamide (6j). According to general procedure 2 from (*R*,*S*)-*N*-(2-benzoyl-4-nitrophenyl)-2-chloro-2-phenylacetamide (2367 mg, 6.0 mmol), *N*-phenylpiperazine (2.75 mL, 18.0 mmol). Purification: chromatography on silica gel (ethyl acetate) to give a yellow solid: yield 2773 mg (89%). ^{1}H NMR (400 MHz, $CDCl_3$): $\delta =$ 2.64 (m, 4H), 3.31 (m, 4H), 4.10 (s, 1H), 6.86–6.89 (m, 3H), 7.24–7.43 (m, 7H), 7.54–7.77 (m, 5H), 8.37–8.47 (m, 2H), 8.89–8.91 (m, 1H), 12.24 ppm (s, 1H).

(*R*,*S*)-*N*-(4-Amino-2-benzoylphenyl)-2-(4-phenyl-1-piperazinyl)-2-phenylacetamide (7j). According to general procedure 3 from (*R*,*S*)-*N*-(2-benzoyl-4-nitrophenyl)-2-(4-phenyl-1-piperazinyl)-2-phenylacetamide (2700 mg, 5.2 mmol) and tin(II)-chloride-dihydrate (5.6 g, 26.0 mmol). Yellow solid: yield 2117 mg (83%). ^{1}H NMR (400 MHz, $CDCl_3$): $\delta = 2.53$ (m, 4H), 3.18 (m, 4H), 3.63 (s, 2H), 3.89 (s, 1H), 6.70–6.79 (m, 5H), 7.14–7.24 (m, 5H), 7.33–7.41 (m, 4H), 7.51–7.53 (m, 1H), 7.68–7.70 (m, 2H), 8.19–8.21 (m, 1H), 11.17 ppm (s, 1H).

(*E*)-(*R*,*S*)-*N*-{3-Benzoyl-4-[2-(4-phenyl-piperazinyl)-2-phenylacetylamino]phenyl}-3-[5-(4-nitrophenyl)-2-furyl]acrylic acid amide

(8j). According to general procedure 1 from (*E*)-3-[5-(4-nitrophenyl)-2-furyl]acrylic acid chloride (260 mg, 1.0 mmol), and (*R,S*)-*N*-(4-amino-2-benzoylphenyl)-2-(4-phenyl-1-piperazinyl)-2-phenylacetamide (491 mg, 1.0 mmol). Yellow solid: yield 222 mg (30%); mp 178 °C; IR (KBr): $\tilde{\nu}$ = 3420, 3058, 2957, 1692, 1624, 1598, 1551, 1512, 1448, 1402, 1331, 1294, 1251, 1179, 852, 753, 694 cm^{-1}; ^1H NMR (500 MHz, [D_6]DMSO): δ = 3.12 (s, 4H), 3.57 (s, 4H), 5.35 (s, 1H), 6.84 (d, J = 16 Hz), 6.87–7.28 (m, 7H), 7.36–8.08 (m, 16H and d, J = 16 Hz, 1H), 8.29–8.31 (m, 1H), 10.80 (s, 1H), 11.51 ppm (s, 1H); MS (ESI): *m/z* 732 (100, $[M+H]^+$), 591 (38), 577 (10), 279 (29). Anal. ($C_{44}H_{37}N_5O_6$) C, H, N.

(*R,S*)-*N*-(2-Benzoyl-4-nitrophenyl)-2-(4-benzyl-1-piperazinyl)-2-phenylacetamide (6k). According to general procedure 2 from (*R,S*)-*N*-(2-benzoyl-4-nitrophenyl)-2-chloro-2-phenylacetamide (2367 mg, 6.0 mmol), *N*-benzylpiperazine (3.13 mL, 18.0 mmol). Purification: chromatography on silica gel (ethyl acetate) to give a light brown solid: yield 480 mg (15%). ^1H NMR (400 MHz, $CDCl_3$): δ = 2.51 (s, 8H), 3.51 (m, 2H), 4.04 (s, 1H), 7.18–7.41 (m, 11H), 7.57–7.81 (m, 4H), 8.37–8.45 (m, 2H), 8.85–8.88 (m, 1H), 12.11 ppm (s, 1H).

(*R,S*)-*N*-(4-Amino-2-benzoylphenyl)-2-(4-benzyl-1-piperazinyl)-2-phenylacetamide (7k). According to general procedure 3 from (*R,S*)-*N*-(2-benzoyl-4-nitrophenyl)-2-(4-benzyl-1-piperazinyl)-2-phenylacetamide (428 mg, 0.8 mmol) and tin(II)-chloride-dihydrate (0.9 g, 4.0 mmol). Yellow solid: yield 400 mg (99%). ^1H NMR (400 MHz, $CDCl_3$): δ = 2.39 (s, 8H), 3.43 (s, 2H), 3.54 (m, 2H), 3.92 (s, 1H), 7.25–7.53 (m, 15H), 7.80–7.83 (m, 2H), 8.24–8.26 (m, 1H), 11.16 ppm (s, 1H).

(*E*)-(*R,S*)-*N*-{3-Benzoyl-4-[2-(4-benzyl-1-piperazinyl)-2-phenylacetylamino]phenyl}-3-[5-(4-nitrophenyl)-2-furyl]acrylic acid amide (8k). According to general procedure 1 from (*E*)-3-[5-(4-nitrophenyl)-2-furyl]acrylic acid chloride (208 mg, 0.8 mmol) and (*R,S*)-*N*-(4-amino-2-benzoylphenyl)-2-(4-benzyl-1-piperazinyl)-2-phenylacetamide (404 mg, 0.8 mmol). Yellow solid: yield 63 mg (11%); mp 181 °C; IR (KBr): $\tilde{\nu}$ = 3420, 2956, 1669, 1624, 1597, 1511, 1448, 1403, 1331, 1290, 1251, 1197, 1179, 1108, 871, 851, 752, 699 cm^{-1}; ^1H NMR (400 MHz, [D_6]DMSO): δ = 3.50 (s, 8H), 4.28 (s, 2H), 4,29 (s, 1H), 6.78 (d, J = 16 Hz, 1H), 7.04–7.05 (m, 1H), 7.26–7.57 (m, 15H and d, J = 16 Hz, 1H), 7.72–7.74 (m, 2H), 7.88–8.00 (m, 4H), 8.31–8.34 (m, 2H), 10.62 (s, 1H), 11.01 ppm (s, 1H); MS (CI): *m/z* 746 (100, $[M+H]^+$), 592 (48), 547 (33), 333 (33), 279 (16), 266 (14). Anal. ($C_{45}H_{39}N_5O_6$) C, H, N.

(*R,S*)-2-Bromo-(4-chlorophenyl)acetic acid (9). According to general procedure 4 from 4-chlorophenylacetic acid (1700 mg, 10.0 mmol), bromine (0.54 mL, 10.5 mmol), and phosphortrichloride (0.1 mL, 1.15 mmol). White solid: yield 1641 mg (66%). ^1H NMR (500 MHz, [D_6]DMSO): δ = 5.80 (s, 1H), 7.42–7.60 (m, 4H), 13.24 ppm (s, 1H).

(*R,S*)-*N*-(2-Benzoyl-4-nitrophenyl)-2-bromo-(4-chlorophenyl)acetamide (10). According to general procedure 1 from (*R,S*)-2-bromo-(4-chlorophenyl)acetic acid (1497 mg, 6.0 mmol) and 2-amino-5-nitrobenzophenone (1453 mg, 6.0 mmol). Purification: recrystallization from ethanol to give a yellow solid: yield 1189 mg (42%). ^1H NMR (400 MHz, $CDCl_3$): δ = 5.49 (s, 1H), 7.21–7.77 (m, 9H), 8.38–8.55 (m, 2H), 8.85–8.88 (m, 1H), 11.95 ppm (s, 1H).

(*R,S*)-*N*-(2-Benzoyl-4-nitrophenyl)-2-(4-chlorophenyl)-2-(4-methyl-1-piperazinyl)acetamide (11). According to general procedure 2 from (*R,S*)-*N*-(2-benzoyl-4-nitrophenyl)-2-bromo-2-(4-chlorophenyl)-acetamide (2463 mg, 5.2 mmol) and *N*-methylpiperazine (1.73 mL, 15.6 mmol). Purification: chromatography on silica gel (ethyl acetate) to give a yellow solid: yield 856 mg (33%). ^1H NMR (500 MHz, $CDCl_3$): δ = 2.04 (s, 4H), 2.10 (s, 3H), 2.38 (s, 4H), 4.06 (s, 1H), 7.27–7.32 (m, 4H), 7.59–7.79 (m, 5H), 8.37–8.48 (m, 2H), 8.85–8.87 (m, 1H), 12.15 ppm (s, 1H).

(*R,S*)-*N*-(4-Amino-2-benzoylphenyl)-2-(4-chlorophenyl)-2-(4-methyl-1-piperazinyl)acetamide (12). According to general procedure 3 from (*R,S*)-*N*-(2-benzoyl-4-nitrophenyl)- 2-(4-chlorophenyl)-2-(4-methyl-1-piperazinyl)acetamide (838 mg, 1.7 mmol) and tin(II)-chloride-dihydrate (1.91 g, 8.5 mmol). Yellow solid: yield 714 mg (91%). ^1H NMR (500 MHz, $CDCl_3$): δ = 2.04 (s, 3H), 2.31 (s, 4H), 2.65 (s, 4H), 3.66 (s, 2H), 3.91 (s, 1H), 7.21–7.39 (m, 6H), 7.50–7.79 (m, 5H), 8.23–8.25 (m, 1H), 11.16 ppm (s, 1H).

(*E*)-(*R,S*)-*N*-{3-Benzoyl-4-[2-(4-chlorophenyl)-2-(4-methyl-1-piperazinyl)acetylamino]phenyl}-3-[5-(4-nitrophenyl)-2-furyl]acrylic acid amide (13). According to general procedure 1 from (*E*)-3-[5-(4-nitrophenyl)-2-furyl]acrylic acid chloride (338 mg, 1.3 mmol) and (*R,S*)-*N*-(4-amino-2-benzoylphenyl)-2-(4-chlorophenyl)-2-(4-methyl-1-piperazinyl)acetamide (602 mg, 1.3 mmol). Yellow solid: yield 331 mg (36%); mp 193 °C; IR (KBr): $\tilde{\nu}$ = 3418, 2959, 1645, 1625, 1598, 1541, 1509, 1489, 1405, 1333, 1288, 1252, 1196, 1180, 1119, 1109, 1092, 1015, 969, 872, 852, 792 cm^{-1}; ^1H NMR (500 MHz, [D_6]DMSO): δ = 2.41 (s, 4H), 2,62 (s, 3H), 2.95 (s, 2H), 3.18 (s, 2H), 4.17 (s, 1H), 6.69 (d, J = 16 Hz, 1H), 7.16–7.69 (m, 13H and d, J = 16 Hz, 1H), 7.79–7.94 (m, 3H), 8.23–8.25 (m, 2H), 10.30 (s, 1H), 10.60 ppm (s, 1H), MS (ESI): *m/z* 706 (50, $[M+H]^+$), 704 (100, $[M+H]^+$), 657 (14), 588 (15), 563 (59), 333 (61), 279 (56), 243 (30), 233 (18), 185 (18), 175 (31). Anal. ($C_{39}H_{34}ClN_5O_6$) C, H, N.

(*R,S*)-2-Bromo-3-(4-chlorophenyl)propionic acid (14). According to general procedure 4 from 3-(4-chlorophenyl)propionic acid (1846 mg, 10.0 mmol), bromine (0.54 mL, 10.5 mmol), and phosphortrichloride (0.1 mL, 1.15 mmol). White solid: yield 1096 mg (72%). ^1H NMR (500 MHz, [D_6]DMSO): δ = 3.17 (m, 2H), 5.44 (dd, J = 9 Hz, J = 6 Hz, 1H), 7.37–7.46 (m, 2H), 7.53–7.65 (m, 2H), 12.49 ppm (s, 1H).

(*R,S*)-*N*-(2-Benzoyl-4-nitrophenyl)-2-bromo-3-(4-chlorophenyl)-propionamide (15). According to general procedure 1 from (*R,S*)-2-bromo-3-(4-chlorophenyl)propionic acid (1844 mg, 76.0 mmol) and 2-amino-5-nitrobenzophenone (1695 mg, 7.0 mmol). Brown oil: yield 2695 mg (79%). The substance was used for further synthesis without purification and characterization.

(*R,S*)-*N*-(2-Benzoyl-4-nitrophenyl)-3-(4-chlorophenyl)-2-(4-methyl-1-piperazinyl)propionamide (16). According to a variation from general procedure 2 from (*R,S*)-*N*-(2-benzoyl-4-nitrophenyl)-2-bromo-3-(4-chlorophenyl)propionamide (2683 mg, 5.5 mmol), *N*-methylpiperazine (1.89 mL, 16.5 mmol), $NaHCO_3$ (1385 mg, 5.5 mmol), and molecular sieve. Purification: chromatography on silica gel (ethyl acetate and ethanol) to give a yellow solid: yield 780 mg (28%). ^1H NMR (400 MHz, [D_6]DMSO): δ = 2.10 (s, 3H), 2.32 (s, 8H), 2.52 (m, 1H), 2.82 (m, 1H), 3.86 (t, J = 7 Hz, 1H), 7.20–7.55 (m, 7H), 7.63–7.85 (m, 3H), 8.07–8.08 (m, 1H), 8.37–8.38 (m, 1H), 11.01 ppm (s, 1H).

(*R,S*)-*N*-(4-Amino-2-benzoylphenyl)-3-(4-chlorophenyl)-2-(4-methyl-1-piperazinyl)propionamide (17). According to general procedure 3 from (*R,S*)-*N*-(2-benzoyl-4-nitrophenyl)-3-(4-chlorophenyl)-2-(4-methyl-1-piperazinyl)propionamide (760 mg, 1.5 mmol) and tin(II)-chloride-dihydrate (1.69 g, 7.5 mmol). Yellow solid: yield 433 mg (61%). ^1H NMR (500 MHz, $CDCl_3$): δ = 2.17 (s, 3H), 2.44 (s, 8H), 2.52 (m, 1H), 3.01 (m, 1H), 3.70 (s, 2H), 3.86 (t, J = 7 Hz, 1H), 6.75–6.86 (m, 2H), 7.11–7.35 (m, 3H), 7.44–7.75 (m, 5H,), 7.97–7.98 (m, 1H), 8.37–8.38 (m, 1H), 10.38 ppm (s, 1H).

(*E*)-(*R*,*S*)-*N*-{3-Benzoyl-4-[3-(4-chlorophenyl)-2-(4-methyl-1-piperazinyl)propionylamino]phenyl}-3-[5-(4-nitrophenyl)-2-furyl]acrylic acid amide (18). According to general procedure 1 from (*E*)-3-[5-(4-nitrophenyl)-2-furyl]acrylic acid chloride (198 mg, 0.9 mmol) and (*R*,*S*)-*N*-(4-amino-2-benzoylphenyl)-3-(4-chlorophenyl)-2-(4-methyl-1-piperazinyl)propionamide (429 mg, 0.9 mmol). Yellow solid: yield 76 mg (12%); mp 168 °C; IR (KBr): $\tilde{\nu}$ = 3418, 2956, 1651, 1622, 1597, 1552, 1511, 1447, 1403, 1331, 1288, 1244, 1198, 1190, 970, 852 cm^{-1}; ^1H NMR (500 MHz, [D_6]DMSO): δ = 2.70 (s, 3H), 2.94 (m, 2H), 3.49 (s, 8H), 4.47 (s, 1H), 6.73 (d, J = 16 Hz, 1H), 6.98–6.99 (m, 1H), 7.22–7.50 (m, 6H and d, J = 16 Hz, 1H), 7.55–7.72 (m, 6H), 7.80–7.81 (m, 1H), 7.93–7.95 (m, 2H), 8.26–8.27 (m, 2H), 10.52 (s, 1H), 11.06 ppm (s, 1H), MS (ESI): *m/z* 720 (15, $[M+H]^+$), 718 (23, $[M+H]^+$), 608 (30), 577 (11), 418 (8), 265 (100), 223 (30). Anal. ($C_{40}H_{36}ClN_5O_6$) C, H, N.

(*R*,*S*)-*N*-(2-Benzoyl-4-nitrophenyl)-2-[(2-dimethylaminoethyl)methylamino]-2-phenylacetamide (19). According to a variation from general procedure 2 from (*R*,*S*)-*N*-(2-benzoyl-4-nitrophenyl)-2-chloro-2-phenylacetamide (2367 mg, 6.0 mmol) and *N*,*N*,*N*′-trimethylethan-1,2-diamine (2.3 mL, 18.0 mmol). Purification: chromatography on silica gel (ethyl acetate) to give a yellow solid: yield 928 mg (34%). ^1H NMR (500 MHz, $CDCl_3$): δ = 2.03 (s, 6H), 2.41 (s, 3H), 2.52 (m, 4H), 4.19 (s, 1H), 7.26–7.38 (m, 5H), 7.53–7.56 (m, 2H), 7.65–7.68 (m, 1H), 7.76–7.78 (m, 2H), 8.34–8.42 (m, 2H), 9.81–8.83 (m, 1H), 12.06 ppm (s, 1H).

(*R*,*S*)-*N*-(4-Amino-2-benzoylphenyl)-2-[(2-dimethylaminoethyl)-methylamino]-2-phenylacetamide (19 reduced). According to general procedure 3 from (*R*,*S*)-*N*-(2-benzoyl-4-nitrophenyl)-2-[(2-dimethylaminoethyl)methylamino]-2-phenylacetamide (921 mg, 2.0 mmol) and tin(II)-chloride-dihydrate (2.25 g, 10.0 mmol). Orange solid: yield 855 mg (99%). ^1H NMR (500 MHz, $CDCl_3$): δ = 2.11 (s, 6H), 2.20 (s, 3H), 2.52 (m, 4H), 3.60 (s, 2H), 4.04 (s, 1H), 6.75–6.84 (m, 2H), 7.21–7.28 (m, 3H), 7.36–7.38 (m, 2H), 7.43–7.49 (m, 2H), 7.57–7.60 (m, 1H), 7.70–7.79 (m, 2H), 8.20–8.22 (m, 1H), 11.15 ppm (s, 1H).

(*E*)-(*R*,*S*)-*N*-(3-Benzoyl-4-{2-[(2-dimethylaminoethyl)methylamino]-2-phenyl-acetylamino}phenyl)-3-[5-(4-nitrophenyl)-2-furyl]-acrylic acid amide (20). According to general procedure 1 from (*E*)-3-[5-(4-nitrophenyl)-2-furyl]acrylic acid chloride (286 mg, 1.1 mmol) and (*R*,*S*)-*N*-(4-amino-2-benzoylphenyl)-2-[(2-dimethylaminoethyl)methylamino]-2-phenylacetamide (476 mg, 1.1 mmol). Yellow solid: yield 696 mg (95%); mp 161 °C; IR (KBr): $\tilde{\nu}$ = 3433, 2958, 1684, 1623, 1597, 1516, 1404, 1332, 1291, 1252, 1180, 852 cm^{-1}; ^1H NMR (400 MHz, [D_6]DMSO): δ = 2.68 (s, 9H), 3.55 (s, 4H), 5.32 (s, 1H), 6.80 (d, J = 16 Hz, 1H), 7.04–7.05 (m, 1H), 7.37–7.55 (m, 9H and d, J = 16 Hz, 1H), 7.65–7.68 (m, 1H), 7.77–7.81 (m, 4H), 7.98–8.00 (m, 2H), 8.31–8.33 (m, 2H), 10.70 (s, 1H), 10.99 ppm (s, 1H), MS (ESI): *m/z* 672 (100, $[M+H]^+$), 531 (93), 431 (11). Anal. ($C_{39}H_{37}N_5O_6$) C, H, N.

(*R*,*S*)-*N*-(2-Benzoyl-4-nitrophenyl)-2-(4-chlorophenyl)[(2-dimethylaminoethyl)methylamino]acetamide (21). According to a variation from general procedure 2 from (*R*,*S*)-*N*-(2-benzoyl-4-nitrophenyl)-2-brom-2-(4-chlorophenyl)acetamide (2842 mg, 6.0 mmol) and *N*,*N*,*N*′-trimethylethan-1,2-diamone (2.3 mL, 18.0 mmol). Purification: chromatography on silica gel (ethyl acetate) to give a yellow solid: yield 989 mg (33%). ^1H NMR (500 MHz, $CDCl_3$): δ = 2.07 (s, 6H), 2.27 (s, 3H), 2.51 (m, 4H), 4.21 (s, 1H), 7.28–7.31 (m, 4H), 7.53–7.56 (m, 2H), 7.65–7.68 (m, 1H), 7.75–7.77 (m, 2H), 8.34–8.37 (m, 1H), 8.41–8.42 (m, 1H), 8.78–8.80 (m, 1H), 12.04 ppm (s, 1H).

(*R*,*S*)-*N*-(4-Amino-2-benzoylphenyl)-2-(4-chlorophenyl)-2-[(2-dimethylaminoethyl)methylamino]acetamide (21 reduced). According to general procedure 3 from (*R*,*S*)-*N*-(2-benzoyl-4-nitrophenyl)-2-(4-chlorophenyl)-[(2-dimethylaminoethyl)methylamino]acetamide (965 mg, 1.95 mmol) and tin(II)-chloride-dihydrate (2.19 g, 9.75 mmol). Orange solid: yield 906 mg (100%). ^1H NMR (500 MHz, $CDCl_3$): δ = 2.14 (s, 6H), 2.19 (s, 3H), 2.51 (m, 4H), 3.61 (s,), 4.06 (s, 1H), 6.76–6.77 (m, 1H), 6.84–6.86 (m, 1H), 7.24–7.33 (m, 4H), 7.44–7.49 (m, 2H), 7.58–7.61 (m, 1H), 7.77–7.78 (m, 2H), 8.17–8.18 (m, 1H), 11.13 ppm (s, 1H).

(*E*)-(*R*,*S*)-*N*-(3-Benzoyl-4-{2-(4-chlorophenyl)-2-[(2-dimethylaminoethyl)methylamino]acetylamino}phenyl)-3-[5-(4-nitrophenyl)-2-furyl]acrylic acid amide (22). According to general procedure 1 from (*E*)-3-[5-(4-nitrophenyl)-2-furyl]acrylic acid chloride (312 mg, 1.2 mmol) and (*R*,*S*)-*N*-(4-amino-2-benzoylphenyl)-2-(4-chlorophenyl)-2-[(2-dimethylaminoethyl)methylamino]acetamide (558 mg, 1.2 mmol). Yellow solid: yield 783 mg (92%); mp 170 °C; IR (KBr): $\tilde{\nu}$ = 3407, 2959, 1684, 1623, 1597, 1516, 1403, 1332, 1247, 1180, 1108, 852 cm^{-1}; ^1H NMR (500 MHz, [D_6]DMSO): δ = 2.71 (s, 3H), 2.80 (s, 6H), 3.55 (s, 4H), 5.43 (s, 1H), 6.82 (d, J = 16 Hz, 1H), 7.02–7.03 (m, 1H), 7.37 (d, J = 16 Hz, 1H), 7.43–7.52 (m, 8H), 7.57–7.59 (m, 1H), 7.62–7.80 (m, 3H), 7.88–7.93 (m, 1H), 7.98–8.00 (m, 2H), 8.30–8.32 (m, 2H), 10.72 (s, 1H), 11.30 ppm (s, 1H), MS (ESI): *m/z* 708 (54, $[M+H]^+$), 706 (100, $[M+H]^+$), 565 (19), 467 (9), 465 (22). Anal. ($C_{39}H_{36}ClN_5O_6$) C, H, N.

***N*-(2-Benzoyl-4-nitrophenyl)-2-[(3-dimetylaminopropyl)methylamino]-2-phenyl-acetamide.** From *N*-(2-*b*enzoyl-4-nitrophenyl)-2-chloro-2-phenylacetamide (2369 mg, 6.0 mmol) and *N*,*N*,*N*′-trimethylpropane-1,3-diamine (697 mg, 6.0 mmol) according to general procedure 2. Purification: column chromatography (ethyl acetate) to give a yellow solid: yield 907 mg (34%); ^1H NMR (500 MHz, [D_6]DMSO): δ = 2.23 (s, 4H), 2.31–2.45 (m, 9H), 3.38 (m, 3H), 7.53–7.70 (m, 8H), 8.36–8.38 (m, 2H), 8.44–8.45 (m, 2H), 8.86–8.88 (d, J = 16 Hz, 1H), 12.13 ppm (s, 1H).

(*R*,*S*)-*N*-(4-Amino-2-benzoylphenyl)-2-(phenyl)-2-[(dimethylaminopropyl)methylamino]acetamide. From *N*-(2-*b*enzoyl-4-nitrophenyl)-2-[(3-dimetylaminopropyl)methylamino]-2-phenylacetamide. (907 mg, 2.04 mmol) and tin(II)chloride-dihydrate (2290 mg, 2.04 mmol) according to general procedure 3. Yellow solid: yield 634 mg (66%); ^1H NMR (500 MHz, [D_6]DMSO) δ = 1.64–1.69 (m, 2H), 2.02–2.09 (m, 7H), 2.23–2.29 (m, 3H), 2.31–2.37 (m, 4H), 3.45 (s, 1H), 3.53 (s, 2H), 6.71 (s, 1H), 7.25–7.71 (m, 11H), 8.20–8.22 (d, J = 16 Hz, 1H), 11.18 (s, 1H).

(*E*)-(*R*,*S*)-*N*-(3-Benzoyl-4-{2-[(3-dimethylaminopropyl)methylamino]-2-phenyl-acetylamino}phenyl)-3-[5-(4-nitrophenyl)-furan-2-yl]acrylic acid amide (23). According to general procedure 1 from (*E*)-3-[5-(4-nitrophenyl)-2-furyl]acrylic acid chloride (576 mg, 1.3 mmol) and (*R*,*S*)-*N*-(4-amino-2-benzoylphenyl)-2-phenyl-[(2-dimethylaminopropyl)-methylamino]acetamide (337 mg, 1.3 mmol). Yellow solid: yield 397 mg (44%); mp 177 °C; IR (KBr): $\tilde{\nu}$ = 3407, 2956, 2704, 1661, 1623, 1597, 1512, 1448, 1332, 1293, 1246 cm^{-1}. ^1H NMR (500 MHz, [D_6]DMSO): δ = 2.30 (s, 2H), 2.64–2.90 (m, 13H), 5.30 (s, 1H), 6.81–6.84 (d, J = 16 Hz, 1H), 7.42–7.69 (m, 12H), 7.80–8.02 (m, 6H), 8.32–8.33 (m, 2H), 10.53 (s, 1H), 10.69 ppm (s, 1H). FAB+ (HRMS): Anal. Calcd for $C_{40}H_{39}N_5O_6$: 686.2979; found: 686.2968.

***N*-(2-Benzoyl-4-nitrophenyl)-2-(4-chlorophenyl)-2-[(3dimethylaminopropyl)methylamino]acetamide.** From *N*-(2-*b*enzoyl-4-nitrophenyl)-2-chloro-2-phenylacetamide (2842 mg, 6 mmol) and *N*,*N*,*N*′-trimethylpropane-1,3-diamine (697 mg, 6.0 mmol) according to general procedure 2. Purification: column chromatography (ethyl acetate) to give a yellow solid: yield 1099 mg (36%). ^1H NMR (500 MHz, $CDCl_3$): δ = 1.74–1.75 (m, 2H), 2.10 (s, 6H), 2.22–2.45 (m,

7H), 4.14 (s, 1H), 7.53–7.76 (m, 9H), 8.36–8.45 (m, 2H), 8.84–8.86 (m, 1H), 12.1 (s, 1H).

(*R*,*S*)-*N*-(4-Amino-2-benzoylphenyl)-2-(4-chlorophenyl)-2-[(dimethylaminopropyl)methylamino]acetamide. From *N*-(2-benzoyl-4-nitrophenyl)-2-[(3-dimetylaminopropyl)methylamino]-2-phenylacetamide (1099 mg, 2.16 mmol) and tin(II)chloride-dihydrate (2430 mg, 2.16 mmol) according to general procedure 3. Yellow solid: yield 628 mg (64%); ^{1}H NMR (500 MHz, [D$_6$]DMSO): $\delta = 1.72$–1.74 (m, 2H), 2.13–2.19 (m, 9H), 2.40–2.48 (m, 3H), 3.61 (s, 2H), 4.00 (s, 1H), 6.70–6.87 (m, 2H), 7.23–7.35 (m, 6H), 7.46–7.49 (m, 2H), 7.75–7.77 (m, 2H), 8.24–8.25 (d, $J = 16$ Hz, 1H), 11.24 (s, 1H).

(*E*)-(*R*,*S*)-*N*-(3-Benzoyl-4-{2-(4-chlorophenyl)-2-[(3-dimethylaminopropyl)methylamino]acetylamino}phenyl)-3-[5-(4-nitrophenyl)-furan-2-yl]acrylic acid amide (24). According to general procedure 1 from (*E*)-3-[5-(4-nitrophenyl)-2-furyl]acrylic acid chloride (368 mg, 1.42 mmol) and (*R*,*S*)-*N*-(4-amino-2-benzoylphenyl)-2-(4-chlorophenyl)-[(2-dimethylaminopropyl)methylamino]acetamide (680 mg, 1.42 mmol). Yellow solid: yield 439 mg (42%); mp 172 °C; IR (KBr): $\tilde{\nu} = 3407$, 2918, 2848, 2595, 1692, 1662, 1623, 1597, 1516, 1493, 1332 cm^{-1}; ^{1}H NMR (500 MHz, [D$_6$]DMSO): $\delta = 2.09$ (s, 4H), 2.50 (s, 2H), 2.73–2.90 (m, 6H), 3.03–3.57 (m, 4H), 5.40 (s, 1H), 6.83–6.86 (d, $J = 16$ Hz, 1H), 7.50–7.81 (m, 13H), 7.90–8.04 (m, 3H), 8.32–8.35 (m, 2H), 10.50 (s, 1H), 10.75 ppm (s, 1H); FAB+ (HRMS): Anal. calcd for $C_{40}H_{38}ClN_5O_6$ 720.2542; found: 720.2596.

Enzyme preparation

Yeast farnesyltransferase was used as a fusion to glutathione S-transferase at the N terminus of the β-subunit. The recombinant farnesyltransferase was produced in *Escherichia coli* DH5α grown in LB media containing ampicillin and chloramphenicol for co-expression of pGEX-DPR1 and pBC-RAM2 for farnesyltransferase production.[30] The enzyme was purified by standard procedures with glutathione-agarose beads for selective binding of the target protein.

Farnesyltransferase assay

The assay was conducted as described elsewhere.[29] Farnesylpyrophosphate (FPP) was obtained as a solution of the ammonium salt in methanol 10 mM aqueous NH_4Cl (7:3) from Sigma–Aldrich. Dansyl-Gly-Cys-Val-Leu-Ser (Ds-GCVLS) was custom synthesized by ZMBH, Heidelberg, Germany. The assay mixture (100 μL volume) contained 50 mM Tris/HCl pH 7.4, 5 mM $MgCl_2$, 10 μM $ZnCl_2$, 5 mM dithiothreitol (DTT), 7 μM Ds-GCVLS, 20 μM FPP, and 5 nmol (approximately) yeast GST-farnesyltransferase and 1% of various concentrations of the test compounds dissolved in dimethyl sulfoxide (DMSO). The progress of the enzyme reaction was followed by monitoring the enhancement of the fluorescence emission at 505 nm (excitation 340 nm). The reaction was started by addition of the enzyme and run in a Quartz cuvette held at 30 °C thermostatically. Fluorescence emission was recorded with a Perkin–Elmer LS50B spectrometer. IC_{50} values (concentrations resulting in 50% inhibition) were calculated from initial velocity of three independent measurements of four to five different concentrations of the inhibitor.

Cytotoxicity assay

HeLa (DSM ACC 57) cells were grown in RPMI 1640 culture medium (GIBCO BRL 21875-034) supplemented with 25 μg mL^{-1} gentamicin sulfate (BioWhittaker 17-528Z), and 10% heat inactivated fetal bovine serum (GIBCO BRL 10500-064) at 37 °C in high density polyethylene flasks (NUNC 156340). The test substances were dissolved in DMSO (10 mg mL^{-1}) before being diluted in the cell culture medium (1:200). The adherent HeLa cells were harvested at the logarithmic growth phase after soft trypsinization, using 0.25% trypsin in PBS containing 0.02% EDTA (Biochrom KG L2163). For each experiment approximately 10000 cells were seeded with 0.1 mL RPMI 1640 (GIBCO BRL 21875-034), containing 25 μg mL^{-1} gentamicin sulfate (BioWhittaker 17-528Z), but without HEPES, per well of the 96-well microplates (NUNC 167008). For the cytotoxic assay HeLa cells were preincubated for 48 h without the test substances. The dilutions of the test substances were carried out carefully on the monolayers of HeLa cells after the pre-incubation time. The HeLa cells were further incubated for 72 h at 37 °C in a humidified atmosphere and 5% CO_2. The adherent HeLa cells were fixed with 25% glutaraldehyde and stained with a 0.05% solution of methylene blue for 15 min. After gently washing, the stain was eluted with 0.2 mL of 0.33 N HCl per well. The optical densities were measured at 660 nm in SUNRISE microplate reader (TECAN). For data analysis the Magellan software (TECAN) was used.

Flexible docking

The protein structure was taken from the PDB entry 1QBQ.[22] Ligands and solvent molecules were removed, but the zinc ion and farnesyl diphosphate were included as part of the protein. For use within AutoDock 3.0,[35,36] polar hydrogen atoms were added with the PROTONATE utility from AMBER.[43] AMBER united atom force field charges were assigned,[44] and solvation parameters were added using the ADDSOL utility from AutoDock 3.0. Ligand structures were built in mol2 format, Gasteiger partial atomic charges were assigned,[45] and all bonds except for amides were kept rotatable. Docking runs were performed with the Lamarckian genetic algorithm included in AutoDock 3.0,[46] performing 50 independent runs per ligand, using an initial population of 50 randomly placed individuals, a maximum number of 1.5×10^6 energy evaluations, a mutation rate of 0.02, a crossover rate of 0.80, and an elitism value of 1. Resulting ligand conformations that differ by less than 1 Å rmsd from each other were clustered together and were represented by the solution with the best docking energy.

Keywords: antimalarial agents · farnesyltransferase · malaria · *Plasmodium falciparum* · protein prenylation

[1] A. Wittinghofer, H. Waldmann, *Angew. Chem.* **2000**, *112*, 4360–4383; *Angew. Chem. Int. Ed.* **2000**, *39*, 4192–4214.
[2] A. D. Cox, C. J. Der, *Curr. Opin. Pharmacol.* **2002**, *2*, 388–393.
[3] J. E. Head, S. R. D. Johnston, *Expert Opin. Emerging Drugs* **2003**, *8*, 163–178.
[4] F. Caponigro, M. Casale, J. Bryce, *Expert Opin. Invest. Drugs* **2003**, *12*, 943–954.
[5] T. B. Brunner, S. M. Hahn, A. K. Gupta, R. J. Muschel, W. G. McKenna, E. Bernhard, *J. Cancer Res.* **2003**, *63*, 5656–5668.
[6] K. Zhu, A. D. Hamilton, S. M. Sebti, *Curr. Opin. Invest. Drugs* **2003**, *4*, 1428–1435.
[7] C.-Y. Huang, L. Rokosz, *Expert Opin. Ther. Pat.* **2004**, *14*, 175–186.
[8] S. M. Sebti, A. A. Adjei, *Semin. Oncol.* **2004**, *31 Suppl. 1*, 28–39.
[9] I. M. Bell, *J. Med. Chem.* **2004**, *47*, 1869–1878.
[10] H.-W. Fu, P. J. Casey, *Recent Prog. Horm. Res.* **1999**, *54*, 315–343.
[11] R. Roskoski, Jr., *Biochem. Biophys. Res. Commun.* **2003**, *303*, 1–7.
[12] D. Chakrabarti, T. Azam, C. DelVecchio, L. Qiu, Y. Park, C. M. Allen, *Mol. Biochem. Parasitol.* **1998**, *94*, 175–184.
[13] D. Chakrabarti, T. Da Silva, J. Barger, S. Paquette, H. Patel, S. Patterson, C. M. Allen, *J. Biol. Chem.* **2002**, *277*, 42066–42073.

[14] K. Yokoyama, P. Trobridge, F. S. Buckner, W. C. Van Voorhis, K. D. Stuart, M. H. Gelb, *J. Biol. Chem.* **1998**, *273*, 26497–26505.
[15] F. S. Buckner, K. Yokoyama, L. Nguyen, A. Grewal, H. Erdjument-Bromage, P. Tempst, C. L. Strickland, L. Xiao, W. C. Van Voorhis, M. H. Gelb, *J. Biol. Chem.* **2000**, *275*, 21870–21876.
[16] K. Yokoyama, P. Trobridge, F. S. Buckner, J. Scholten, K. D. Stuart, W. C. Van Voorhis, M. H. Gelb, *Mol. Biochem. Parasitol.* **1998**, *94*, 87–97.
[17] F. S. Buckner, R. T. Eastman, J. L. Nepumuceno-Silva, E. C. Speelmon, P. J. Myler, W. C. Van Voorhis, K. Yokoyama, *Mol. Biochem. Parasitol.* **2002**, *122*, 181–188.
[18] M. Ibrahim, N. Azzouz, P. Gerold, R. T. Schwarz, *Int. J. Parasitol.* **2001**, *31*, 1489–1497.
[19] M. Kumagai, A. Makioka, T. Takeuchi, T. Nozaki, *J. Biol. Chem.* **2003**, *279*, 2316–2323.
[20] J. Sachs, P. Malaney, *Nature* **2002**, *415*, 680–685.
[21] R. G. Ridley, *Nature* **2002**, *415*, 686–693.
[22] C. L. Strickland, W. T. Windsor, R. Syto, L. Wang, R. Bond, R. Wu, J. Schwartz, H. V. Le, L. S. Beese, P. C. Weber, *Biochemistry* **1998**, *37*, 16601–16611.
[23] M. Schlitzer, *Curr. Pharm. Des.* **2002**, *8*, 1713–1722.
[24] J. Wiesner, A. Mitsch, P. Wißner, O. Krämer, H. Jomaa, M. Schlitzer, *Bioorg. Med. Chem. Lett.* **2002**, *12*, 2681–2683.
[25] J. Wiesner, K. Kettler, J. Sakowski, R. Ortmann, H. Jomaa, M. Schlitzer, *Bioorg. Med. Chem. Lett.* **2003**, *13*, 361–363.
[26] J. Wiesner, K. Fucik, K. Kettler, J. Sakowski, R. Ortmann, H. Jomaa, M. Schlitzer, *Bioorg. Med. Chem. Lett.* **2003**, *13*, 1539–1541.
[27] J. Wiesner, A. Mitsch, H. Jomaa, M. Schlitzer, *Bioorg. Med. Chem. Lett.* **2003**, *13*, 2159–2161.
[28] The in vitro and in vivo antimalarial activities of inhibitors **8d** and **13** have been reported in a preliminary communication: J. Wiesner, K. Kettler, J. Sakowski, R. Ortmann, A. M. Katzin, E. A. Kimura, K. Silber, G. Klebe, H. Jomaa, M. Schlitzer, *Angew. Chem.* **2004**, *116*, 254–257; *Angew. Chem. Int. Ed.* **2004**, *43*, 251–254.
[29] D. L. Pompliano, R. P. Gomez, N. J. Anthony, *J. Am. Chem. Soc.* **1992**, *114*, 7945–7946.
[30] K. Del Villar, H. Mitsuzawa, W. Yang, I. Sattler, F. Tamanoi, *J. Biol. Chem.* **1997**, *272*, 680–687.
[31] R. E. Desjardins, C. J. Canfield, J. D. Haynes, J. D. Chulay, *Antimicrob. Agents Chemother.* **1979**, *16*, 710–718.
[32] W. Trager, J. B. Jensen, *Science* **1976**, *193*, 673–675.
[33] M. L. Ancelin, M. Calas, J. Bompart, G. Cordina, D. Martin, M. B. Bari, T. Jei, P. Druilhe, H. Vial, *J. Blood* **1998**, *91*, 1426–1437.
[34] W. Peters in *Malaria, Vol. 1* (Ed.: J. P. Kreier), Academic Press, New York, **1980**, pp. 160–161.
[35] D. S. Goodsell, A. J. Olson, *Proteins Struct. Funct. Genet.* **1990**, *8*, 195–202.
[36] G. M. Morris, D. S. Goodsell, R. Huey, A. J. Olson, *J. Comput.-Aided Mol. Des.* **1996**, *10*, 293–304.
[37] B. Boeckmann, A. Bairoch, R. Apweiler, M.-C. Blatter, A. Estreicher, E. Gasteiger, M. J. Martin, K. Michoud, C. O'Donovan, I. Phan, S. Pilbout, M. Schneider, *Nucleic Acids Res.* **2003**, *31*, 365–370.
[38] C. Notredame, D. Higgins, J. Heringa, *J. Mol. Biol.* **2000**, *302*, 205–217.
[39] M. A. Marti-Renom, A. Stuart, A. Fiser, R. Sánchez, F. Melo, A. Sali, *Annu. Rev. Biophys. Biomol. Struct.* **2000**, *29*, 291–325.
[40] I. C. Moura, G. Wunderlich, M. L. Uhrig, A. S. Couto, V. J. Peres, A. M. Katzin, E. A. Kimura, *Antimicrob. Agents Chemother.* **2001**, *45*, 2553–2558.
[41] M. Böhm, A. Mitsch, P. Wißner, I. Sattler, M. Schlitzer, *J. Med. Chem.* **2001**, *44*, 3117–3124.
[42] K. Kettler, J. Wiesner, K. Silber, P. Haebel, R. Ortmann, I. Sattler, H. M. Dahse, H. Jomaa, G. Klebe, M. Schlitzer, *Eur. J. Med. Chem.* **2005**, *40*, 93–101.
[43] D. A. Case, D. A. Pearlman, J. W. Caldwell, T. E. Cheatham III; J. Wang, W. S. Ross, C. L. Simmerling, T. A. Darden, K. M. Merz, R. V. Stanton, A. L. Cheng, J. Vincent, M. Crowley, V. Tsui, H. Gohlke, R. J. Radmer, Y. Duan, J. Pitera, I. Massova, G. L. Seibel, U. C. Singh, P. K. Weiner, P. A. Kollman, **2002**, AMBER 7; University of California, San Francisco (USA).
[44] S. J. Weiner, P. A. Kollman, D. A. Case, U. C. Singh, C. Ghio, G. Alagona, S. Profeta, P. Weiner, *J. Am. Chem. Soc.* **1984**, *106*, 765–784.
[45] J. Gasteiger, M. Marsili, *Tetrahedron* **1980**, *36*, 3219–3228.
[46] G. M. Morris, D. S. Goodsell, R. S. Halliday, R. Huey, W. E. Hart, R. K. Belew, A. J. Olson, *J. Comput. Chem.* **1998**, *19*, 1639–1662.
[47] M. Schlitzer, *Curr. Med. Chem.: Anti-Infect. Agents* **2005**, *4*, 277–286.
[48] M. P. Glenn, S.-Y. Chang, O. Hucke, C. L. M. J. Verlinde, K. Rivas, C. Horný, K. Yokoyama, F. S. Bruckner, P. R. Pendyala, D. Chakrabarti, M. Gelb, W. C. Van Voorhis, S. M. Sebti, A. D. Hamilton, *Angew. Chem.* **2005**, *117*, 4981–4984; *Angew. Chem. Int. Ed. Engl.* **2005**, *44*, 4903–4906.
[49] M. P. Glenn, S.-Y. Chang, C. Horný, K. Yokoyama, E. E. Pusateri, S. Fletcher, C. G. Cummings, F. S. Buckner, P. R. Pendyala, D. Chakrabarti, S. M. Sebti, M. Gelb, W. C. Van Voorhis, A. D. Hamilton, *J. Med. Chem.* **2006**, *49*, 5710–5727.
[50] A. Ryckebusch, P. Gilleron, R. Millet, R. Houssin, A. Lemoine, N. Pommery, P. Grellier, C. Sergheraert, J.-P. Henichart, *Chem. Pharm. Bull.* **2005**, *53*, 1324–1326.
[51] L. Nallan, K. D. Bauer, P. Bendale, K. Rivas, K. Yokoyama, C. P. Horney, P. Rao Pedyala, D. Floyd, L. J. Lombardo, D. K. Williams, A. Hamilton, S. Sebti, W. T. Windsor, P. C. Weber, F. S. Buckner, D. Chakrabarti, M. H. Gelb, W. C. Van Voorhis, *J. Med. Chem.* **2005**, *48*, 3704–3713.
[52] W. C. Van Voorhis, K. L. Rivas, P. Bendale, L. Nallan, C. Horney, L. K. Barrett, K. D. Bauer, B. P. Smart, S. Ankala, O. Hucke, C. L. M. J. Verlinde, D. Chakrabarti, C. Strickland, K. Yokoyama, F. S. Buckner, A. D. Hamilton, D. K. Williams, L. J. Lombardo, D. Floyd, M. H. Gelb, *Antimicrob. Agents Chemother.* **2007**, *51*, 3659–3671.
[53] V. J. Bulbule, L. Rivas, C. L. M. J. Verlinde, W. C. Van Voorhis, M. H. Gelb, *J. Med. Chem.* **2008**, *51*, 384–387.
[54] M. I. Esteva, K. Kettler, C. Maidana, L. Fichera, A. M. Ruiz, E. J. Bontempi, B. Andersson, H.-M. Dahse, P. Haebel, R. Ortmann, G. Klebe, M. Schlitzer, *J. Med. Chem.* **2005**, *48*, 7186–7191.

Received: February 18, 2008
Revised: April 10, 2008
Published online on May 9, 2008

